J-Researchers

Journal of Civil Engineering Researchers

Journal homepage: www.journals-researchers.com

The Effect of Using Fly Ash with Various Additives on the Microstructure and Compressive Strength of Self-Compacting Concrete (Review Study)

Meysam gholami,[a] Omid Hassanshahi,[b]

[a] *Department of Civil Engineering, University of Guilan, Rasht, Iran*
[b] *ARISE, ISISE, Department of Civil Engineering, University of Minho, 4800-058 Guimarães, Portugal*

ABSTRACT

This review article provides a comprehensive investigation into the effects of utilizing fly ash (FA) along with other mineral additives such as metakaolin (MK), silica fume (SF), hydrated lime (HL), and others on the properties of Self-Compacting Concrete (SCC). The primary objective of this study is to analyze and synthesize existing research on the simultaneous influence of various chemical additives and fly ash on the microstructure and compressive strength of self-compacting concrete. Recognized for its ease of implementation and enhanced performance, self-compacting concrete is considered an advanced technology in the concrete industry, and the use of mineral additives, particularly fly ash, can contribute to the improvement of its mechanical properties and durability.The methodology of these studies primarily involves examining the concrete microstructure using Scanning Electron Microscopy (SEM) and evaluating the compressive strength of concrete specimens at different ages. Results indicate that partial replacement of cement with activated fly ash (using sodium hydroxide) can reduce the hydration process while enhancing pozzolanic reactions, leading to improved strength properties. The optimal performance of activated fly ash-based SCC, in terms of strength, was observed at 10% to 15% replacement. SEM images revealed that fly ash particles are spherical, whereas activated fly ash particles are angular and elongated, which contributes to improved concrete matrix density and reduced porosity, thereby increasing compressive strength.Furthermore, studies on concrete containing mineral additives demonstrated that MK provides higher initial strength compared to other additives. This study concludes that the use of fly ash and other mineral additives, particularly in combination with activators or hydrated lime, can effectively enhance the mechanical and microstructural properties of self-compacting concrete, making it a sustainable and efficient option for construction applications. This review also underscores the importance of a profound understanding of the relationship between material composition, microstructure, and mechanical properties for the optimal formulation of SCC.

ARTICLE INFO

Received: October 30,2025
Accepted: January 25,2026

Keywords:
Self-Compacting Concrete (SCC)
Fly Ash
Compressive Strength
Mineral addition
Scanning Electron Microscopy (SEM)
Interfacial Transition Zone (ITZ)

DOI: 10.61186/JCER.8.1.16
DOR: 20.1001.1.22516530.1399.11.4.1.1

1. Introduction

Self-Compacting Concrete (SCC) is recognized as a milestone in concrete technology due to its improved performance and more favorable working conditions. Over the years, SCC has been introduced as the most advanced and innovative development in concrete technology. SCC is considered the concrete of the future, as it will ultimately replace traditional concrete due to its inherent advantages. Mineral admixtures are used in this concrete as fillers or partial replacements for cement and aggregates to improve concrete properties and produce environmentally friendly SCC. Among these materials, Fly Ash (FA), as an artificial pozzolan and a by-product of coal-fired industries, holds a

special place. The use of fly ash in self-compacting concrete, in addition to reducing cement consumption and costs, leads to improved workability and flowability, reduced heat of hydration, increased long-term stability, and reduced permeability [1,2]. On the other hand, the use of various admixtures is inevitable to achieve specific properties and overcome certain challenges. When replacing cement with any admixture, it must be noted that microstructural properties are also affected. Simultaneously, these materials can have synergistic or antagonistic effects on the fresh and hardened behavior of concrete [3]. These interactions directly impact the microstructure of concrete, including the distribution and density of the cement paste matrix and the Interfacial Transition Zone (ITZ) between the paste and aggregate. The microstructure, in turn, is the main determining factor for the compressive strength and other mechanical properties of concrete. Therefore, a deep understanding of the relationship between material composition (fly ash and admixtures), microstructure, and mechanical properties is crucial for the optimal formulation of self-compacting concrete [4-6]. The microstructural characteristics of SCC are investigated using advanced laboratory methods. Among these methods, Scanning Electron Microscope (SEM) analysis can be mentioned. The aim of this review article is to summarize, analyze, and present an integrated perspective of conducted research on the simultaneous effect of using fly ash and various chemical admixtures on the two key indicators of microstructure and compressive strength of self-compacting concrete.

2.Research Method

A growing number of researchers use advanced and precise tools for research in the field of self-compacting concrete. Figure 1 shows the results of VOSviewer software. This software for scientometric analysis illustrates the extent of publications and their connections in a specific field of study [7]. As evident in the image generated by this software, in the field of self-compacting concrete (SCC), the most studies have been conducted in the areas of microstructure study, compressive strength, investigation of the ITZ, and related topics. For this reason, in this article, concrete has been studied and analyzed via Scanning Electron Microscopy. Scanning Electron Microscopy (SEM) is used to observe the surface of samples. In this method, electrons are used instead of light to form an image. When the sample surface is irradiated with a narrow electron beam in the SEM, secondary electrons are emitted from the sample surface. These secondary electrons form a two-dimensional image of the sample surface, which is detected by a detector. A comparison was made between the compressive strengths of the mixtures, and its relationship with the concrete microstructure was investigated. The microstructure of the concrete mixtures was analyzed using Scanning Electron Microscopy (SEM), which helps in observing the microstructure of the cement paste and the bond between the cement paste and aggregate. The objective of this study is to analyze the microstructural behavior of fly ash-based self-compacting concretes using the SEM method and their compressive strength through the replacement of concrete components with cost-effective and alternative by-products. Microstructural analysis does not only serve to prove the theory but also aids in understanding the reasons behind the results related to mechanical properties and durability. Therefore, microstructural analysis provides a method for studying the internal structure of concrete. In the following, the studies conducted regarding each of the existing articles in this field have been evaluated, and finally, these materials are compared and analyzed.

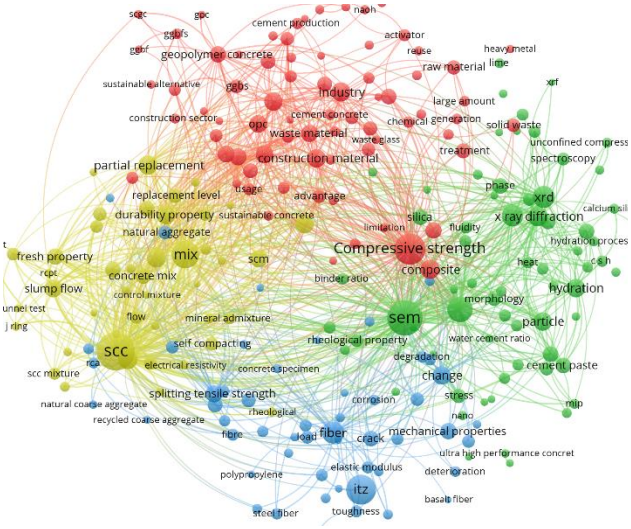

Figure 1. VOSviewer software results.

3.Related articles:

3.1.Fly Ash and Sodium Hydroxide

This study focuses on the structural and composite behavior of self-compacting concrete (SCC) based on fly ash activated with sodium hydroxide (NaOH). Fly ash was partially replaced with ordinary Portland cement from 0 to 30 percent. The tests conducted on concrete samples included workability, strength, microstructure, and impact resistance. The results indicated that activated fly ash reduces the heat of the hydration process in the concrete mixture but enhances pozzolanic reactions, leading to improved strength properties. The addition of activated fly ash modifies the concrete's mineralogy, as evident in its strength characteristics.

The best performance of activated fly ash-based SCC, in terms of strength, was observed at 10 to 15 percent replacement, which can somewhat reduce the production cost of SCC while providing the advantage of enhanced strength. Table 1 shows the nomenclature and mix design of each sample. [8]

Table 1.
Mix proportions

Mix	Cement (kg/m^3)	Fly ash (kg/m^3)	Super plasticizeras (kg/m^3)
SCCF0	470	0	3.76
SCCF10	423	47	3.76
SCCF15	399.5	70.5	3.76
SCCF20	376	94	3.76
SCCF25	352.5	117.5	3.76
SCCF30	329	141	3.76

Water (kg/m^3)=183.3, M-sand (kg/m^3)=962.8, Granite (kg/m^3)=727.84

3.1.1.SEM Analysis

Figure 2 shows the scanning electron microscopy (SEM) images of raw fly ash and activated fly ash. The SEM images revealed that the raw fly ash particles have a spherical shape (Figure 2a), whereas the activated fly ash particles are elongated and angular (Figure 2b), which is a result of continuous burning. SEM images of the concrete are presented in Figure 3.

The structure and porosity of the concrete mixtures differed, and it was found that the pore size of the conventional concrete (Figure 3a) was larger than that of the concrete made with the alkali-activated fly ash mixture with 20% replacement (Figure 3b).

The roundness and smaller particle size were calculated as 2.047, indicating the angularity of the particles, as higher roundness values mean a more angular material [9]. Consequently, better packing between particles was achieved, and porosity in the matrix was reduced. Therefore, the strength of the mixture increased. [8]

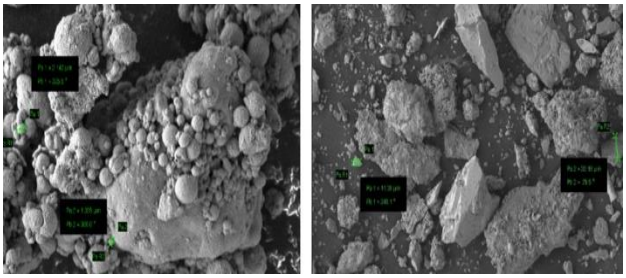

Figure 2. SEM morphology (a) fly ash (b) activated fly ash

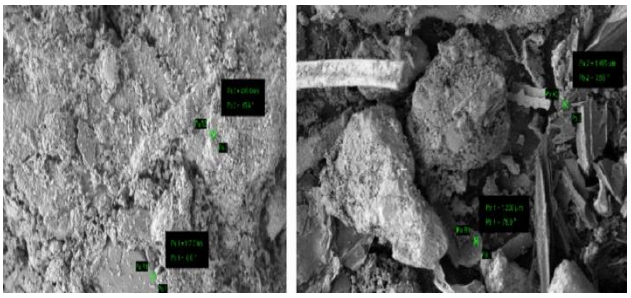

Figure 3. SEM morphology of concrete (a) control (b) 20% activated fly ash concrete.

3.1.2.Compressive Strength

Testing of hardened concrete plays a very important role in controlling and verifying the quality of cementitious concrete operations. The compressive strength test is essential in cases where tensile or shear strength is of higher importance. Figure 4 shows the strength characteristics of the concrete samples. The compressive strength of the cubes (Figure 4) increased with the addition of activated fly ash up to 15%; such that the resulting strength at both 7-day and 28-day intervals was higher than that of the conventional concrete mixture. However, a further increase in the amount of activated fly ash led to a gradual decrease in strength. A decrease in compressive strength at replacements beyond 15% fly ash has also been reported in another study [10]. This reduction might be due to the increased siliceous minerals in the concrete matrix, which reduced the hydration rate without providing a sufficient curing period for the pozzolanic reactions to complete fully. A longer curing process could improve the strength performance of this type of concrete. [8]

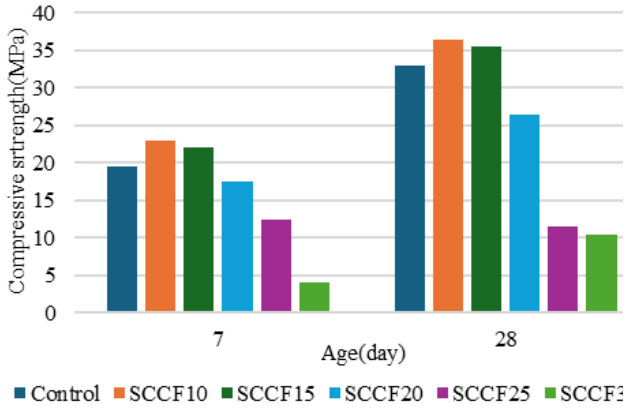

Figure 4. Strength properties of concrete

3.2. Fly Ash, Silica Fume, and Metakaolin at High Temperatures

In this study, SCC was developed using three different admixtures—Fly Ash (FA), Silica Fume (SF), and Metakaolin (MK)—as cementitious materials by replacing cement. The mechanical properties of self-compacting concrete mixed with FA and SF before heating showed similar results, whereas the MK-based SCC exhibited higher strength than the other mixtures. Regarding specimens exposed to high temperatures up to 1000°C, the SCC mixed with MK yielded the lowest residual strength compared to the FA-based and SF-based mixtures. Further microstructural investigations were conducted to examine the internal structure of specimens subjected to different heating temperatures.From the results,it is concluded that the greater the strength gain due to aging (curing), the greater the strength loss due to temperature increase. Table 2 shows the nomenclature and mixdesign of each sample. [11]

Table 2.
Mix proprtions(kg/m^3)

Mix	Cement	Sand	CA	SF/FA/MK	W/C	SP
NCC	360	607.00	1214.00	-	0.5	-
SCC-SF	324	961.17	932.14	36	0.49	4.6
SCC-FA	252	911.63	885.58	108	0.49	5.4
SCC-MK	306	941.35	903.21	54	0.49	4.3

3.2.1.SEM Analysis

Analysis using Scanning Electron Microscopy (SEM) was performed on samples of self-compacting concrete (SCC) containing Fly Ash (FA), Silica Fume (SF), and Metakaolin (MK) that were exposed to different temperatures. Figure 5 shows SEM micrographs of the SCC samples after exposure to temperatures of 500°C, 750°C, and 1000°C. Images 5a, 5b, and 5c show the microstructure of the SCC-FA specimens at 500°C, 750°C, and 1000°C, respectively. Images 5d, 5e, and 5f belong to the SCC-SF specimens, and images 5g, 5h, and 5i are related to the SCC-MK specimens. At higher temperatures, damages such as porosity (voids) and microcracks were observed in the specimens. Notably, all three compositions (SCC containing FA, SF, and MK) developed significant cracking at 500°C. At 750°C, the SEM images indicated changes in the concrete's microstructure, such as increased voids and widening of microcracks in the SCC matrix. These changes were more severe in the SCC-SF and SCC-MK compositions compared to SCC-FA. Furthermore, at this temperature, the amorphous C-S-H gel underwent a phase transformation, chemically bound water was released from the C-S-H gel, and the long chains of the C-S-H gel were broken. At 1000°C, the formation of microcracks, voids, and new phases due to the degradation of the C-S-H gel, along with the release of chemically bound water, were the main reasons for the compressive strength reduction compared to the unheated specimens. [11-14]

3.2.2.Compressive Strength

The specimens were heated and tested at three different curing periods—7, 14, and 28 days—to determine the mechanical properties of the concrete. The compressive strength results are reported as the average of three concrete specimens tested at a specific temperature.

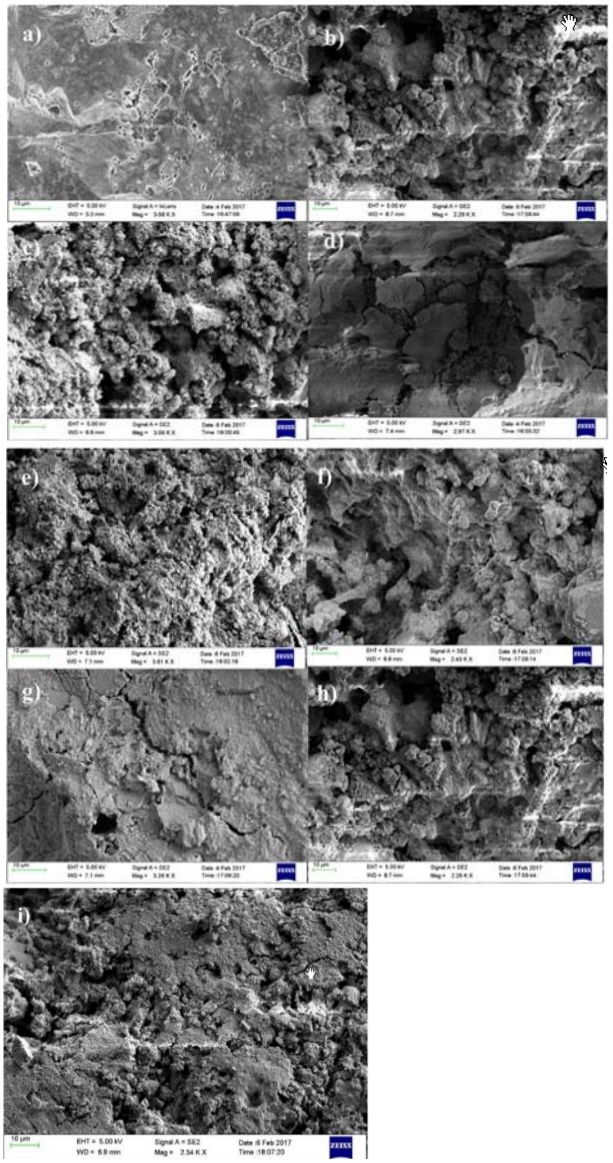

Figure 5. SEM analysis of (a-c) SCC-FA; (d-f) SCC-SF and (g-i) SCC-MK

The initial and residual compressive strength of self-compacting concrete containing Fly Ash (FA) is shown in

Figure 6. The figure indicates that increasing the curing period (from 7 to 28 days) increases the strength, while increasing the temperature reduces the compressive strength of the mixture. In specimens that were water-cured and then exposed to high temperature, a 70% to 80% reduction in strength was observed (Figure 6a). Air-cooled mixtures experienced a 55% to 75% strength reduction, while some air-cooled specimens retained relatively better strength (Figure 6b). The initial compressive strength and strength reduction in self-compacting concrete containing Silica Fume (SF) and Metakaolin (MK) exposed to high temperature are shown in Figures 7 and 8, respectively. Similar to the concrete containing FA, specimens with SF and MK also gained strength with increased curing age and experienced strength loss with increased temperature. The mixture containing SF under AC conditions had a strength reduction of 55% to 75% (Figure 7a), and under WC conditions, it was between 60% and 80% (Figure 7b). The mixture containing MK under AC conditions showed a strength reduction of 65% to 80% (Figure 8a), and under WC conditions, it was between 80% and 85% (Figure 8b). The mixture containing MK achieved the highest initial compressive strength compared to the other mixtures but, in return, suffered the greatest strength loss upon exposure to heat. [11,15]

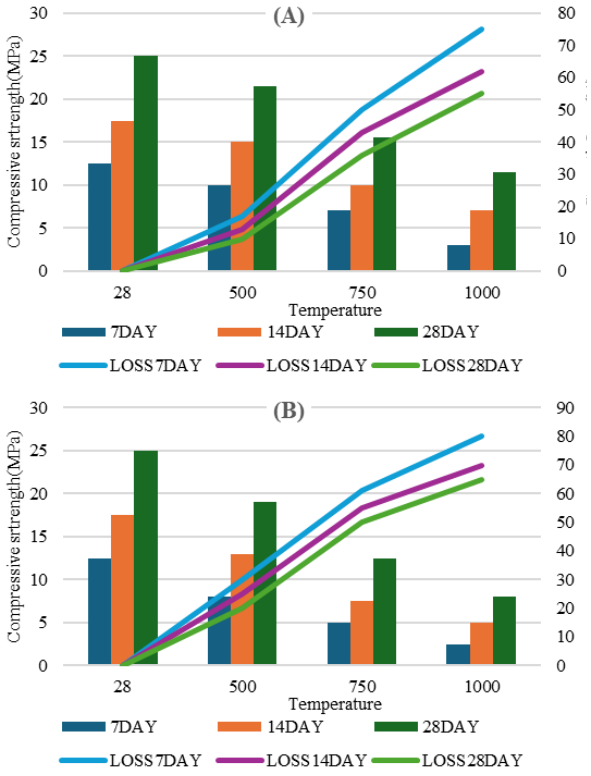

Figure 6. Strength loss of SCC-FA- a) Air-cooled specimens and b) Water-cooled

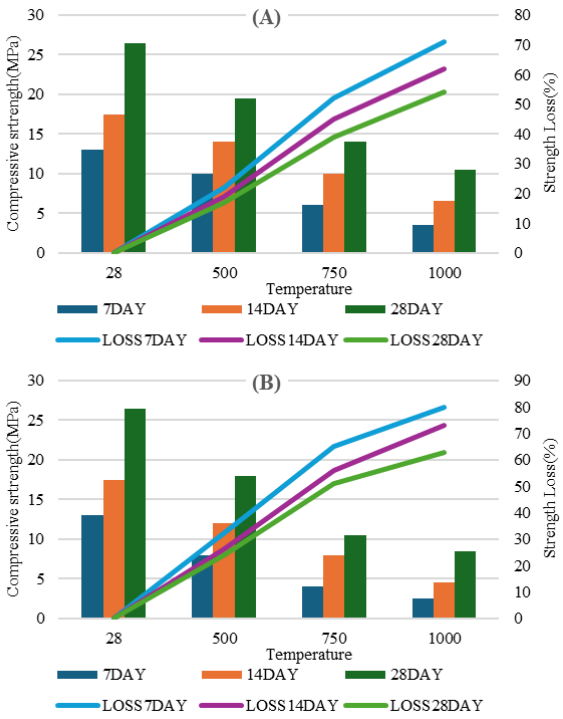

Figure 7. Strength loss of SCC-SF- a) Air-cooled specimens and b) Water-cooled specimens

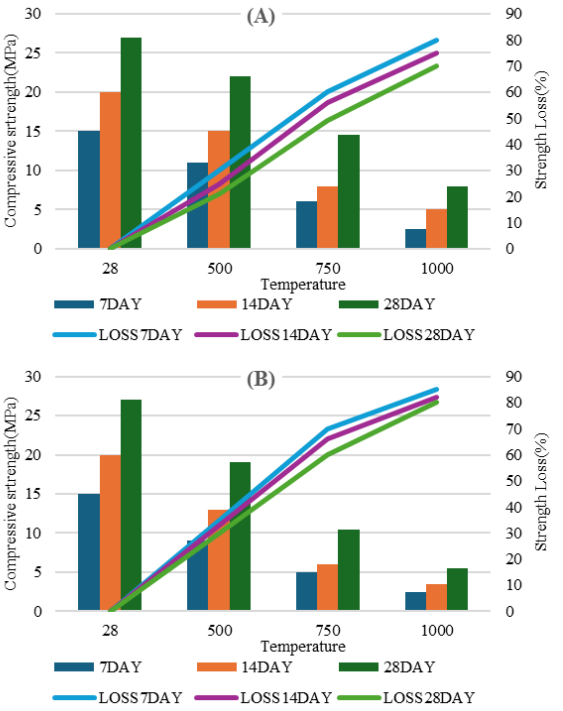

Figure 8. Strength loss of SCC-MK- a) Air-cooled specimens and b) Water-cooled

3.3. Fly Ash, Metakaolin, and Hydrated Lime

This study evaluated the compressive strength and hydration development of self-compacting concrete with reduced cement content (SCC-LC). To achieve this, Portland Cement (PC), Metakaolin (MK), Fly Ash (FA), and Hydrated Lime (HL) were used in binary, ternary, and quaternary cementitious mixtures. Nine SCC mixes were produced according to Table 3: [16]

Table 3.
Concrete compositions (kg/m3).

Mix	PC	FA	MK	HL	SAND	GRAVEL	WATER	SP	FINES	PASTE (L/M^3)	W/B (L/M^3)	%SAND
C500	500	-	-	-	870	880	200	13.0	500	360.3	1.3	49.7
NBC	300	-	-	-	1053	867	180	7.8	*	266.2	1.8	54.8
B500.FA	200	300	-	-	870	880	170	9.0	500	358.1	0.9	49.7
B500.FAHL	200	300	-	25	870	880	170	9.6	525	369.2	0.9	49.7
B500.FAM	150	250	100	-	870	880	170	9.6	500	359.8	0.9	49.7
B500.FAMHL	150	250	100	25	870	880	170	12.3	525	371.0	0.9	49.7
B400.FA	160	240	-	-	1034	916	140	12.4	400	290.5	0.9	53
B400.FAHL	160	240	-	20	1034	916	140	12.4	420	299.4	0.9	53
B400.FAM	120	200	80	-	1034	916	140	13.5	400	291.9	0.9	53
B400.FAMHL	120	200	80	20	1034	916	140	13.5	420	300.8	0.9	53
EFNARC rules	-	-	-	-	-	750-1000	150-210		380-600	300-380	0.85-1.1	48-55

The assessment of compressive strength gain was conducted at 3, 7, 14, 21, 28, and 90 days. Hydration assessment was performed using X-ray Diffraction at 28 days. The obtained results proved the feasibility of producing self-compacting concrete (SCC-LC) with a cement content between 120 and 200 kg/m³ due to the excellent ability of FA and MK to maintain cohesiveness. The compressive strength measured at 28 days for SCC-LC ranged between 25 and 40 MPa, with a cement efficiency of 3.2 to 5.0 kg/m³ per MPa. SEM and X-ray diffraction showed that the main hydrated products formed were Gismondine and C-S-H, and Portlandite was fully consumed in the hydration by 28 days, except in the SCC mixture with FA and HL. [16]

3.3.1.SEM Analysis

The hydration process was evaluated using Scanning Electron Microscopy (SEM). These tests were performed only on the B500 – Low-Cement Self-Compacting Concrete (SCC-LC) specimens. The SEM testing was also conducted using a Nova Nano SEM 200 device. The samples used in this test were also taken from the crushed concrete after the compression test on day 28. In SCC concretes containing HL, it is observed that hydrates such as C-S-H have formed, and calcium sulfoaluminates (Y) and calcium aluminosilicate hydrate (known as Gismondine) (G) are also present. The formation of crystalline calcium aluminosilicate hydrates is due to the extra alumina and silica available from the FA and MK. This phenomenon has been confirmed by other research as well [17]. Figure 9 shows the presence of the Gismondine phase. This phase can form in cementitious systems with high FA and MK content, especially when the Aluminum to Calcium ratio (Al/Ca) in the mix is high. The formation of calcium aluminosilicate at room temperature is facilitated by the high initial pH and the rapid dissolution of amorphous silica and alumina phases [18]. In Figure 9, the SEM micrograph of sample B500.FAM shows the presence of FA, the C-S-H phase, hydrated calcium sulfoaluminates (Y), and Gismondine (G). The morphology of Gismondine in some areas appears as a ball-of-wool-like structure (G), which has been previously reported by Hug et al. [16, 19].

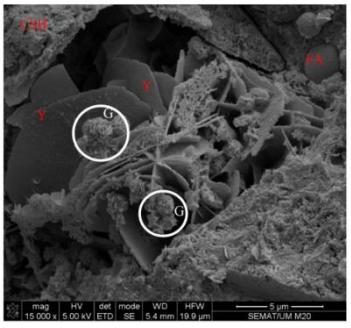

Figure 9. SEM images of B500.FAM after curing at 28 days

3.3.2.Compressive Strength

The compressive strength of the Low-Cement Self-Compacting Concrete (SCC-LC) specimens tested at ages of 3, 7, 14, 21, 28, and 90 days, after curing at 20±2°C, is

shown in Figure 10. As expected, the compressive strength increases over time. The SCC-LC compositions with B500 and B400 ratios at 28 and 90 days exhibited compressive strengths in the ranges of 20-40 MPa and 28-58 MPa, respectively. Even with a very low cement content (between 120 and 200 kg/m³), the obtained compressive strength values confirm the usability of this type of concrete in constructions where the required compressive strength is typically between C20/25 and C30/40.Figure 10 shows that hydrated lime improved the compressive strength of the SCC. The percentage increase in strength for each mix is indicated. The 55.5% increase in compressive strength of the B500FAHLmix is notable, reaching a compressive strength of 58.3 MPa at 90 days, whereas the B500FA mix only achieved 37.5 MPa.Hydrated Lime (HL) had the most significant effect on increasing both early-age and ultimate strength, as the B500 and B400 compositions generally produce low amounts of Portlandite.

According to Figure 10, the strength increase with HL addition is more pronounced when the binder composition consists only of cement and fly ash (FA). Ternary compositions including cement, metakaolin (MK), and FA showed a lower percentage increase in strength, as evident in the B500FAM and B400FAM mixes.

Previous investigations also showed that adding 5% hydraulic lime had a better effect than 3%. Furthermore, MK was found to play a vital role in increasing the early-age strength up to 28 days. SCCs containing only FA (such as B500FA and B400FA), even with higher cement content, had less early-age strength gain compared to mixes containing MK. This indicates the higher reactivity of metakaolin compared to fly ash, which improves the hydration process and fills the microscopic voids in the concrete, consequently increasing the compressive strength.

A comparison between Figures 10(a) and 10(b) shows the positive effect of using MK as a replacement for cement and FA on the 28-day strength. Notably, the B500FAMHL mix contains only 150 kg/m³ of cement, while B500FA contains 200 kg/m³ of cement, yet both achieved a similar compressive strength (~40 MPa). A similar case is observed in Figures 10(c) and 10(d), where the B400FAMHL mix with only 120 kg/m³ of cement reached 27.5 MPa at 28 days, similar to B400FAHL with 160 kg/m³.Considering the cement content, the SCC-LC mixes also demonstrated consistent and environmentally friendly performance in concrete strength development at 28 days. At 90 days, this sustainability characteristic became even more pronounced. [16]

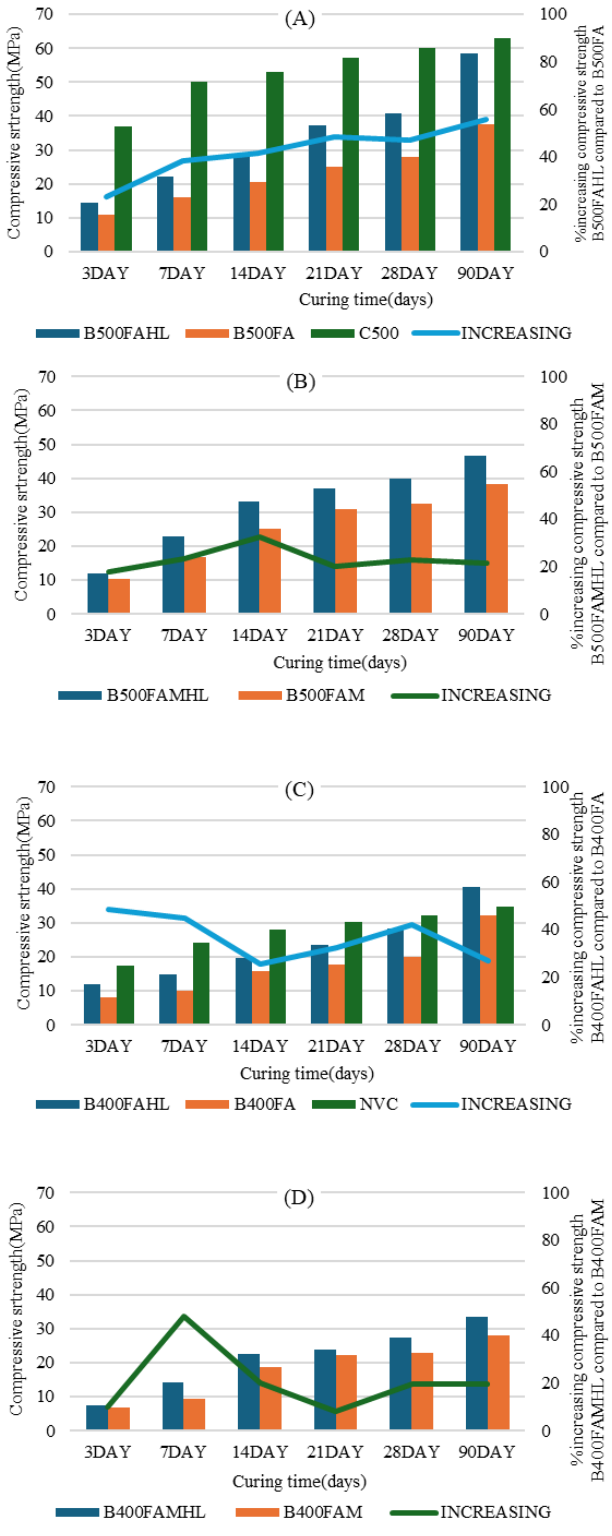

Figure 10. Compressive strength evolution with age

3.4. Fly Ash and Palm Oil Fuel Ash

This article evaluates the feasibility of using Palm Oil Fuel Ash (POFA) and Fly Ash (FA) as replacements for Ordinary Portland Cement (OPC) in Self-Compacting Concretes (SCC). The compressive strength of the self-compacting concrete was determined at 7, 28, and 90 days using cubes and cylinders, and its microstructural properties were identified using Scanning Electron Microscopy (SEM). When comparing POFA and FA, it was found that FA performed better than POFA for equal OPC replacements. Furthermore, the TNY combination showed significant improvement in its microstructural characteristics compared to POFA and FA. The results also indicate that incorporating POFA and FA at higher replacement levels has significant potential for use as medium-strength concrete. Subsequently, DTA shows that the $Ca(OH)_2$ content for all samples with higher replacements at later ages was lower than that of the control sample. It also showed a relationship between $Ca(OH)_2$ and the compressive strength of SCC, which should be useful for forensic investigations indicating the amount of hydrated products in concrete.

The use of the two by-products, palm oil waste ash and coal ash, will lead to a cleaner and more cost-effective waste disposal solution for these industries, as well as benefits for the construction sector. Table 4 shows the nomenclature of each sample. [20]

potential for use as medium-strength concrete. Subsequently, DTA shows that the $Ca(OH)_2$ content for all samples with higher replacements at later ages was lower than that of the control sample. It also showed a relationship between $Ca(OH)_2$ and the compressive strength of SCC, which should be useful for forensic investigations indicating the amount of hydrated products in concrete.

The use of the two by-products, palm oil waste ash and coal ash, will lead to a cleaner and more cost-effective waste disposal solution for these industries, as well as benefits for the construction sector. Table 4 shows the nomenclature of each sample. [20]

Table 4.
SP Content for all SCC mixes..

Mix	SP (kg/m^3)
C	1.10
FA10	0.80
FA20	0.75
FA30	0.66
FA40	0.66
POFA10	1.10
POFA20	1.10
POFA30	1.20
POFA40	1.40
TNY10	1.10
TNY20	1.10
TNY30	1.10
TNY40	1.10

3.4.1.SEM Analysis

Figure 11 shows that the control sample at 90 days has a denser structure with a significant amount of C-S-H gel observed, but only a negligible amount of Calcium Hydroxide (CH) and Ettringite. The C-S-H gel, which has a fibrous appearance, is clearly adhered to the surface of the plate-like CH crystals or to the aggregates, eventually forming larger crystals.

Furthermore, Figure 12 shows that the SCC containing Palm Oil Fuel Ash (POFA) has a network-like structure, likely indicating the presence of secondary C-S-H gel. A very small amount of CH (crystals with higher brightness) is also visible, which is confirmed by the TGA curve (small endothermic peak and mass loss).

The micrograph of SCC containing Fly Ash (FA) in Figure 13 shows a substantial amount of Ettringite, which could be due to the higher amount of Aluminum Oxide (Al_2O_3) in FA (about 20%) compared to POFA (8.9%) or OPC (5.2%).

In Figure 14, it can be observed that the TNY40 sample has formed larger clusters of C-S-H and Ettringite. It can also be seen that these samples are denser than the POFA and FA concretes. Moreover, the lower aluminum oxide content in POFA reduced the Ettringite formation in the TNY concrete. [20]

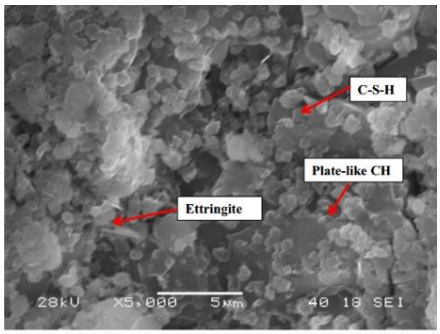

Figure 11. SEM Image for Control SCC at 90 days.

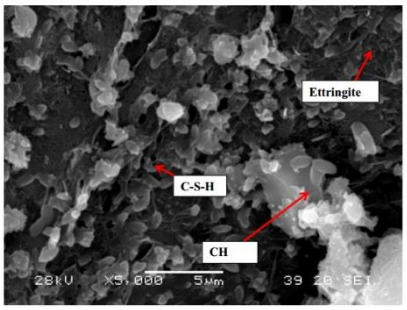

Figure 12. SEM Image for POFA40 at 90 days.

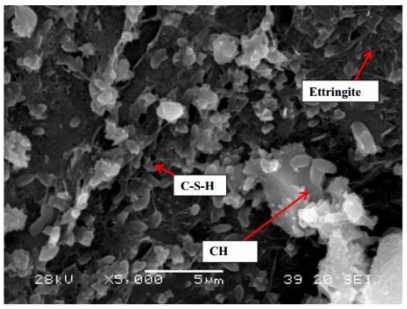

Figure 13 SEM Images for FA40 at 90 days..

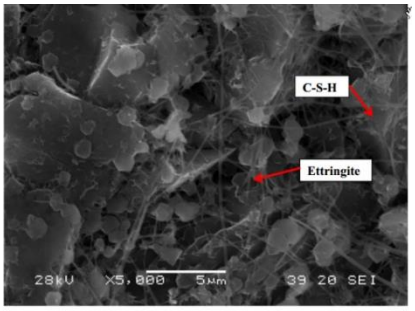

Figure 14. SEM Image for TNY40 at 90 days.

3.4.2.Compressive Strength

As the percentage replacement of Palm Oil Fuel Ash (POFA) and Fly Ash (FA) increases, the compressive strength of binary and ternary self-compacting concretes decreases compared to the control sample. Compared to other materials, the highest recorded compressive strength at similar replacement percentages belonged to concretes containing FA. As observed in Figures 15 to 17, samples with lower replacement percentages (e.g., 10% at 28 days)

had strength similar or equal to the control sample, but at higher replacement percentages, FA had about 1.4 times higher strength than POFA. This indicates that mixes containing POFA weaken the strength gain process in hardened concrete.

In all samples containing SCMs, strength improvement was observed at later ages. This is attributed to the pozzolanic properties and the micro-filling effect of the waste particles. The cube and cylinder compressive strengths of the SCC samples are shown in Figures 15 and 16. Additionally, Figure 17 shows the cylinder-to-cube strength ratio, which falls below the line provided by Domone [21]. The compressive strength systematically improves with age. [20]

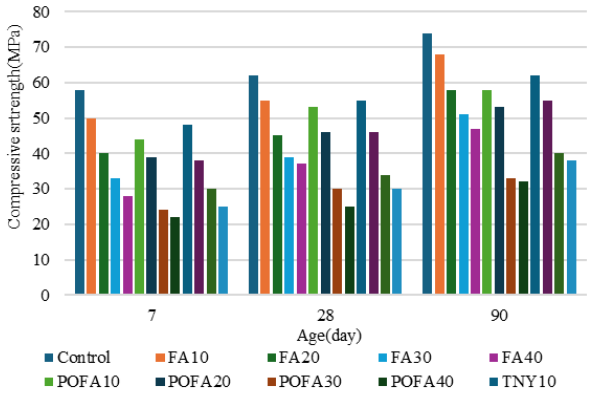

Figure 15. Cylinder compressive strength of SCC incorporating blended POFA and FA.

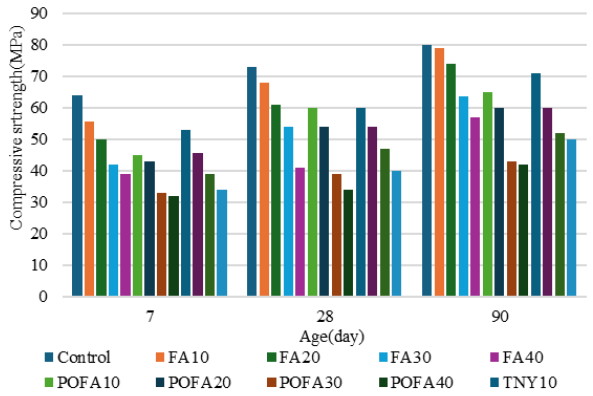

Figure 16. Cube compressive strength of SCC incorporating blended POFA and FA.

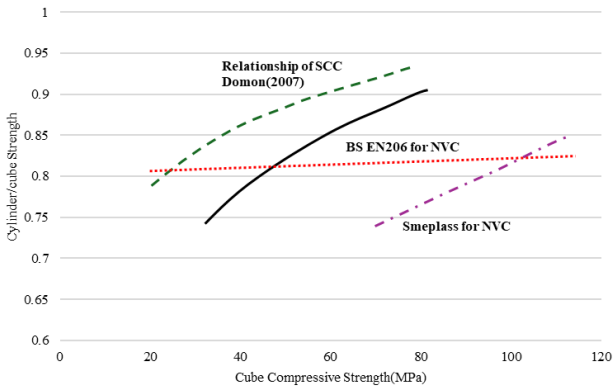

Figure 17. Cube compressive strength vs. cylinder to cube compressive strength ratio.

3.5.Fly Ash and Blast Furnace Slag (Alkali-Activated)

Improving the rheology, morphology, and strength performance of Alkali-Activated Self-Compacting Concretes (SCAAC) incorporating Fly Ash (FA) as a replacement for Ground Granulated Blast Furnace Slag (GBFS) remains challenging. To address this need, five mixes with different amounts of FA (30, 40, 50, 60, and 70% by weight) as a replacement for GBFS were prepared. The produced specimens were thoroughly investigated to examine their textures, microstructures, and strength properties. The various characteristics of the obtained SCAACs were compared with the control mix containing 100% GBFS. The SCAACs prepared with 40, 50, and 60% FA showed improved workability performance (plastic viscosity, passing and filling ability, segregation resistance). Furthermore, the compressive, tensile, and flexural strengths of the SCAACs decreased with increasing FA content. Concrete prepared with 70% FA content showed a weak structure due to the formation of fewer hydration products. The observed reduction in the drying shrinkage of the proposed SCAACs was mainly attributed to the addition of a higher amount of FA in the mix. It has been established that replacing GBFS with FA could be prospective for producing sustainable cement-free self-compacting concretes useful for future-building sectors. Table 5 shows the nomenclature and mix design of each sample. [22]

Table 5.
Mix proprtions(kg/m3)

Mix code	Cement	FA	GBFS	Super plasticizer
OPC	484	-	-	7.26
SCAAC1	-	-	484	0
SCAAC2	-	145.2	338.8	0
SCAAC3	-	193.6	290.4	0
SCAAC4	-	242	242	0
SCAAC5	-	290.4	193.6	0
SCAAC6	-	338.8	145.2	0

Gravel(kg/m^3)=756, Sand(kg/m^3)=844, Water(kg/m^3)=252

3.5.1.SEM Analysis

Figure 18 displays the Scanning Electron Microscopy (SEM) images of four selected Alkali-Activated Fly Ash Concrete (SCAAC) specimens prepared with 0, 30, 50, and 70 percent Fly Ash (FA) as a replacement for Blast Furnace Slag (GBFS). The images clearly show the effect of changing the FA level on the surface texture of the samples.

Figure 18a shows the morphology of the control sample (0% FA). This sample has a denser structure compared to other samples prepared with different FA amounts.

The morphology of the concrete prepared with 30% FA (Figure 18b) indicated the presence of fewer microcracks, micro-pores, and unreacted particles compared to samples prepared with 50 and 70% FA. This led to a reduction in Compressive Strength (CS) in concretes containing more than 30% FA. In Figure 18c, the concrete specimens prepared with 50% FA as a GBFS replacement showed more cracks and pores than the 30% and control samples, which occurred due to the influence of CaO, Al_2O_3, and SiO_2 compounds on the hydration process. The propagation of C-S-H and C-A-S-H gels in the concrete matrix was less extensive with higher FA contents, resulting in structures with weaker bonds compared to samples with lower FA content (30%), which was the reason for the poorer compressive strength performance of these concretes compared to the control sample (0% FA).

The results in Figure 18d show an increase in cracks, roughness, and pores on the sample surfaces when FA was increased to 70%. Indeed, the C-(A)-S-H gels at low FA levels had fully propagated over the sample surfaces, creating a relatively smooth and solid texture.

According to reports [23-25], increasing the FA amount can lead to an increase in the amount of unreacted quartz (SiO_2) in the alkali-activated matrix, resulting in increased porosity and poor morphology. In fact, the strength performance of the proposed concretes was negatively affected by high FA contents. It has been confirmed that increasing the FA content (and simultaneously decreasing the GBFS content) can negatively affect the formulation of C-(A)-S-H gels, leading to the production of semi-reacted gels (such as Mullite) and unreacted particles like quartz. [22,26]

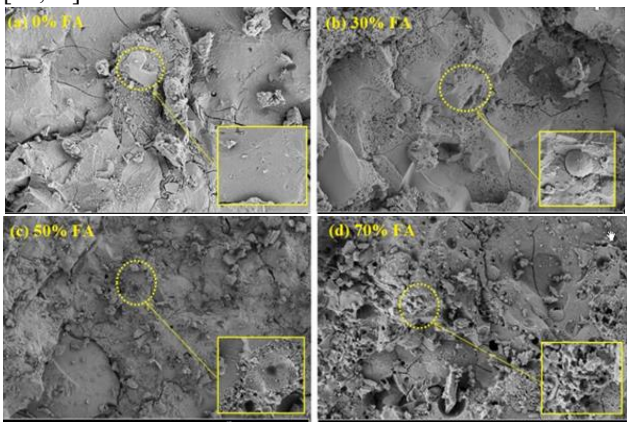

Figure 18. SEM micrographs of the concrete specimens containing FA of (a) 0% (b) 30% (c) 50% and (d) 70%.

3.5.2.Compressive Strength

Figure 19 shows the compressive strength (CS) performance of Alkali-Activated Fly Ash Concretes (SCAACs) prepared with different amounts of Fly Ash (FA) as a replacement for Blast Furnace Slag (GBFS). The concrete specimens were tested at curing ages of 1, 3, 7,

28, 56, and 90 days.Depending on the specimen age, the compressive strength of the control specimens (containing only GBFS) measured between 30 and 70 MPa, whereas this range decreased to 20-55 MPa with an increase in the FA amount (as a GBFS replacement). However, the compressive strength of the SCAAC specimens at both early and later ages was higher than that of ordinary Portland cement (OPC)-based specimens. [22]

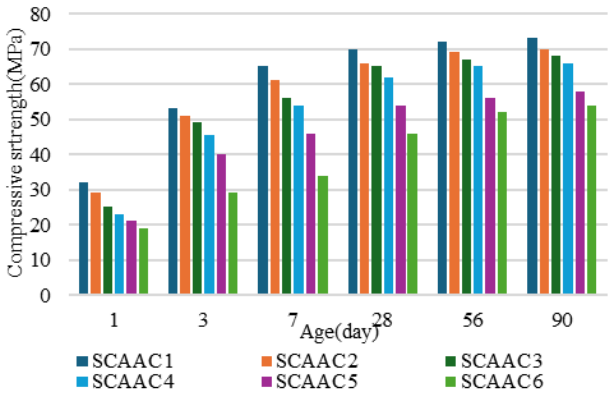

Figure 19. FA contents dependent variation in the CS of the SCAACs cured at different ages.

3.6. Fly Ash, Silica Fume, and Marble Cutting Slurry Waste

The objective of this study is to produce economical and high-efficiency HSSCC using MCSW, Fly Ash (FA), and Silica Fume (SF). This contributes to the beneficial use of MCSW and minimizes the need for using large amounts of cement in HSSCC production, thereby significantly reducing CO2 emissions. A total of sixteen HSSCC mixes, in binary, ternary, and quaternary forms, were prepared by combining MCSW, FA, and SF as cement replacements. Among all HSSCC mixes, one mix with 100% cement binder was prepared and designated as the control mix. Mechanical performance was assessed in terms of compressive strength, and microstructural investigation was conducted using Scanning Electron Microscopy (SEM) and Fourier Transform Infrared (FTIR) techniques. It was observed that the addition of MCSW and FA improved the fresh properties of HSSCC. The combined use of 10% MCSW and 15% FA with 5% SF as cement replacement led to enhanced mechanical performance and improved microstructure. Table 5 shows the nomenclature and mix design of each sample. [27].

3.6.1.SEM Analysis

Scanning Electron Microscopy (SEM) analysis was performed to investigate the changes induced in the microstructure of the concrete mixtures.The SEM image related to the control mix is shown in Figure 20(a). This image shows weak formation of the Interfacial Transition Zone (ITZ) between the paste and aggregates. Also, the presence of voids and cracks leads to its inferior mechanical performance compared to the binary 5SF mix.

In the 5SF mix, a well-formed Interfacial Transition Zone (ITZ) is observed, as visible in Figure 20(b). This image shows a dense paste and fewer voids.The quaternary mix 15FA10M exhibited a very dense paste matrix and the least number of voids, as displayed in Figure 20(c). The appropriate proportioning and uniform distribution of MCSW, FA, SF, and cement resulted in the improved mechanical performance of the concrete. [27]

Table 6.
Quantities of materials in kg to produce one cubic meter HSSCC

Mix	W/P*	WATER	Powder Content(kg/m^3)				Aggregate(kg/m^3)		SP(kg/m^3)
			Cement	Marble powder	Silica fume	Fly Ash	Fine	Coarse	
C-1	0.33	181.5	550	0	0	0	970	722	7.7
5SF	0.33	181.5	522.5	0	27.5	0	970	722	8.25
10M	0.33	181.5	467.5	55	27.5	0	970	722	6.05
20M	0.33	181.5	412.5	110	27.5	0	970	722	4.95
30M	0.33	181.5	357.5	165	27.5	0	970	722	3.575
15FA	0.33	181.5	440	0	27.5	82.5	970	722	3.3
15FA10M	0.33	181.5	385	55	27.5	82.5	970	722	1.925
15FA20M	0.33	181.5	330	110	27.5	82.5	970	722	1.65
15FA30M	0.33	181.5	275	165	27.5	82.5	970	722	1.815
25FA	0.33	181.5	385	0	27.5	137.5	970	722	1.65
25FA10M	0.33	181.5	330	55	27.5	137.5	970	722	1.375
25FA20M	0.33	181.5	275	110	27.5	137.5	970	722	1.1
25FA30M	0.33	181.5	220	165	27.5	137.5	970	722	1.375
35FA	0.33	181.5	330	0	27.5	192.5	970	722	1.21
35FA10M	0.33	181.5	275	55	27.5	192.5	970	722	1.1
35FA20M	0.33	181.5	220	110	27.5	192.5	970	722	1.045

*water to powder ratio(total quantity of cement, MCSW, FA, and SF termed as powder)

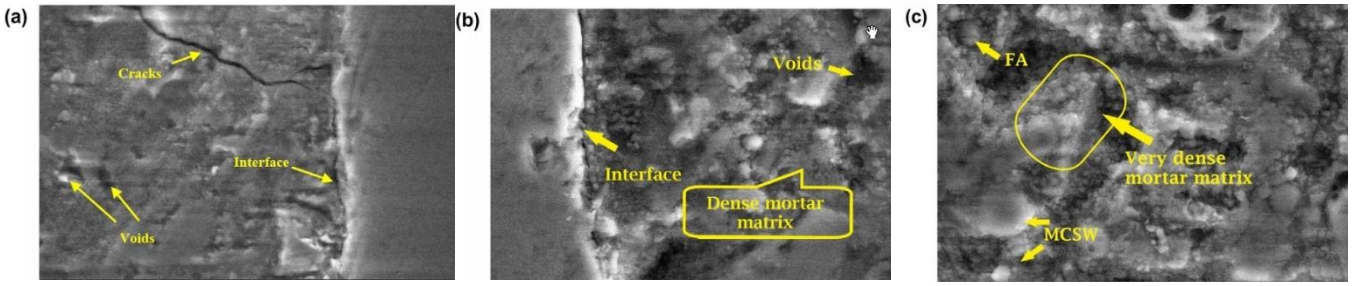

Figure 20. (a). SEM micrograph of control mix, (b). SEM micrograph of 5SF mix, (c). SEM micrograph of 15FA10M mix.

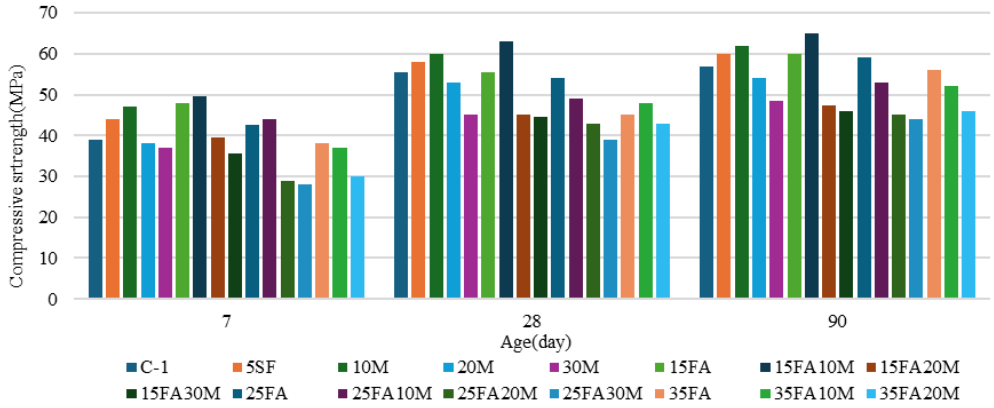

Figure 21. Variation in Compressive strength of HSSCC mixes

3.6.2.Compressive Strength

The results of the compressive strength test are presented graphically in Figure 21. The strength increase in the 5SF mix is due to the micro-filling and pozzolanic effect of Silica Fume (SF).
The results indicate that replacing cement with MCSW (Marble Cutting Slurry Waste) up to 10% in HSSCC yields higher compressive strength than both the control mix and the 5SF mix. The quaternary mix 15FA10M achieved the highest compressive strength compared to all other mixes at 7, 28, and 90 days. [27]

3.7.Fly Ash, Metakaolin, and Blast Furnace Slag

The objective of this study is to investigate the mechanical and microstructural properties of Self-Compacting Concrete (SCC) mixtures containing three Supplementary Cementitious Materials (SCMs): Metakaolin (MK), Ground Granulated Blast Furnace Slag (GGBS), and Fly Ash (FA). For the mixtures, cement was replaced with SCMs at different levels. The mechanical properties were evaluated in comparison to a control mix (without SCMs). The microstructural properties were investigated using SEM and EDS on mixtures with high SCM content. The use of SCMs led to an increase in compressive strength. Metakaolin, as a cement replacement material, had the most significant impact on the mechanical and microstructural properties of SCC at all ages. Table 6 shows the nomenclature and mix design of each sample. [28]

3.7.1.SEM Analysis

Scanning Electron Microscopy (SEM) images were taken of the SCC mixtures with the highest content of Supplementary Cementitious Materials (SCMs) to examine the microstructural characteristics of the Interfacial Transition Zone (ITZ) and the paste surrounding the aggregates. The SEM images for mixtures containing 20% Metakaolin (MK) and 30% GGBS with two different water-to-binder ratios (w/b) are shown in Figures 22 and 23. Figure 22 shows SEM images of SCC mixtures containing 20% by weight of MK with two w/b ratios. Figure 22-a displays a drier structure compared to the same mix with a w/b ratio of 0.45 (Figure 22-b). This indicates that MK, in the presence of more water, is capable of

producing a higher volume of C-S-H gel; meaning MK acts more actively in the presence of excess water.

Table 7.
Mix proprtions(kg/m3)

Mix COD	PC	MK	GGBS	FA	SP
Group 1, w/b=0.4,sand=802.9,gravel=877.2,lime=89.4,water160					
40C	400	-	-	-	4.5
40M10	360	40	-	-	8.6
40M20	320	80	-	-	10.4
40G10	360	-	40	-	5.3
40G20	320	-	80	-	6.1
40G30	280	-	120	-	6.5
40F10	360	-	-	40	3.9
40F20	320	-	-	80	3.3
40F30	280	-	-	120	3.6
Group 2, w/b=0.45,sand=732.5,gravel=851.7,lime=121.6,water=180					
45C	400	-	-	-	4.3
45M10	360	40	-	-	7.9
45M20	320	80	-	-	9.6
45G10	360	-	40	-	4.9
45G20	320	-	80	-	5.3
45G30	280	-	120	-	5.8
45F10	360	-	-	40	3.6
45F20	320	-	-	80	3.1
45F30	280	-	-	120	2.3

However, according to the compressive strength results in Figures 2 to 4, these two mixes have nearly the same compressive strength. This suggests that for high MK contents, the concrete's flowability can be improved by increasing the water content without having a negative impact on compressive strength.

Figure 23 shows SEM images of SCC mixtures containing 30% by weight of GGBS with two w/b ratios. It is observed that there is a significant difference between the paste of these two mixtures. The SCC mix with 30% GGBS and a w/b ratio of 0.45 (Figure 23-b) has a more uniform paste compared to the same mix with a w/b ratio of 0.40 (Figure 23-a). The greater paste uniformity is related to the higher water volume, but no difference in the amount of C-S-H gel is observed between the two mixes. This confirms that more water does not affect the increased production of C-S-H gel in GGBS. Furthermore, the type of cracking present in the 40G30 mix (Figure 23-a) is more critical than the cracking in the 45G30 mix (Figure 23-b), which is another reason for the importance of paste uniformity, as it directly affects the quality of the transition zone.In general, based on the SEM images presented in Figures 22 and 23, it can be confirmed that MK has a greater effect on strengthening the microstructure of the transition zone compared to GGBS. This finding is consistent with previous studies conducted by Asbridge and Page .[29] [28]

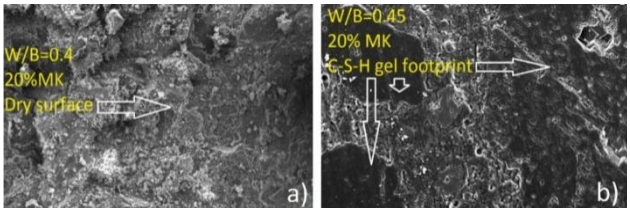

Figure 22. SEM pictures of 40M20 (a) and 45M20 (b).

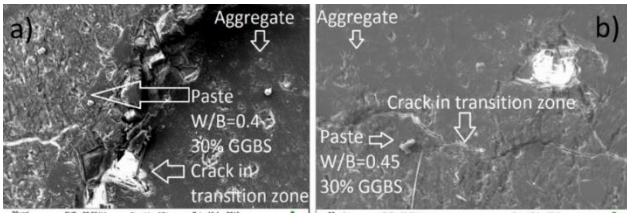

Figure 23. SEM pictures of 40G30 (a) and 45G30 (b).

3.7.2.Compressive Strength

The compressive strength of all Self-Compacting Concrete (SCC) mixtures at 7, 28, and 56 days for two water-to-binder ratios (w/b) is displayed in Figures 24, 25, and 26. It is observed that mixes with a higher percentage replacement of Metakaolin (MK) achieved higher compressive strength for both w/b ratios. The SCC concrete with 20% Metakaolin showed exceptionally high compressive strength at all ages, particularly 77.7 MPa at 7 days with a w/b ratio of 0.4.The increase in early-age strength of mixes containing MK is primarily due to the rapid pozzolanic reaction of metakaolin. This pozzolanic activity is related to the high silica content (about 25%) in metakaolin, which improves the formation of C-S-H gel in fresh concrete and enhances the properties of hardened concrete at both early and later ages.

Also, the high specific surface area of MK particles increases their reactivity.The SCC mixtures containing Ground Granulated Blast Furnace Slag (GGBS) with a w/b ratio of 0.4 also showed a significant increase in compressive strength at all ages as the GGBS replacement percentage increased. Compared to the control mix, all GGBS mixes had lower strength at 7 days; however, the 30% GGBS replacement performed better after 28 days. Moreover, all GGBS mixes with a w/b ratio of 0.45 achieved higher compressive strength than the control mix at all ages. The SCC mixtures containing Fly Ash (FA) showed lower strength than the control mix at all ages; although, the compressive strength of these mixes increased with a higher FA replacement level. [28]

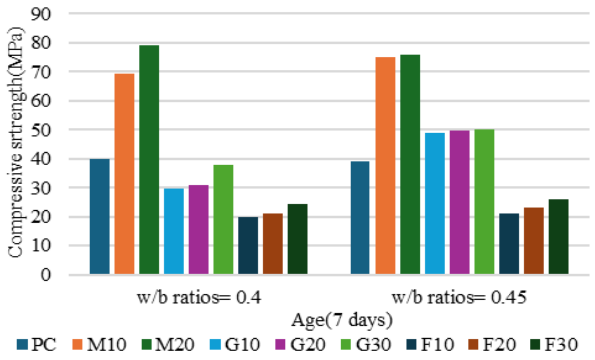

Figure 24. Compressive strength of SCC for both w/b ratios at 7days.

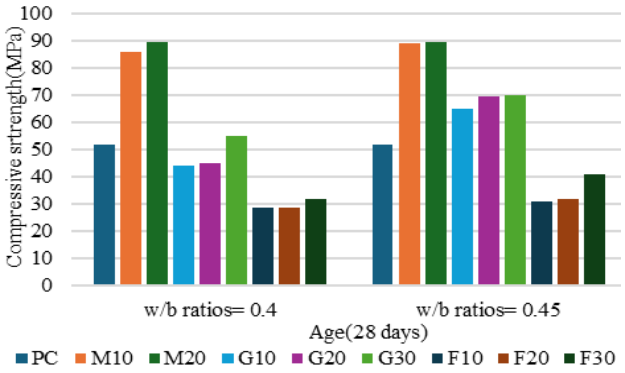

Figure 25.Compressive strength of SCC for both w/b ratios at28 days

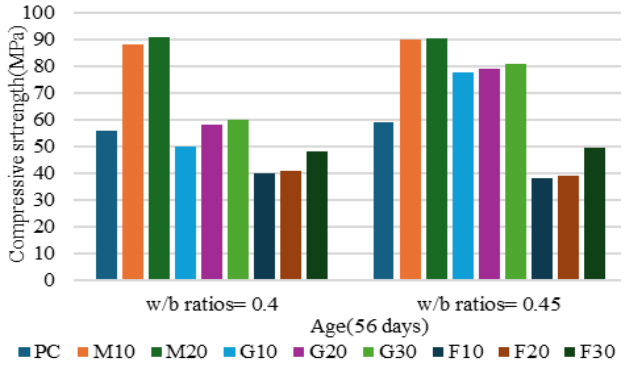

Figure 26.Compressive strength of SCC for both w/b ratios at56 days

3.8. Fly Ash Microspheres and Phosphorous Slag Powder

Self-compacting concrete with two types of pozzolanic admixtures, namely Fly Ash Microspheres (FB) and Phosphorous Slag Powder (PS), was studied in this research. The mechanical properties and durability of self-compacting concrete with different admixtures were investigated. The results showed that the workability of the concrete was optimal when FB and PS were added at 15% each. While the early-age mechanical properties were not as good as the control specimens, their long-term strength exceeded that of the control with increased curing time. Meanwhile, XRD, TGA-DTG, and SEM tests were conducted on specimens cured for 7 and 28 days. SEM testing confirmed that the excellent filling property and pozzolanic effect of FB alter the interfacial bonding between cement particles. Mercury intrusion porosimetry tests indicated that the volume of internal pores decreases with the addition of FB and PS. Table 7 shows the nomenclature and mix design of each sample. [30]

Table 8.
Mix proportion of the specimens.

Mix design code	System	Weight of constituents kg/m^3 of concrete		
		C	FB	PS
Control	OPC	346	-	-
CFB-5%	OPC+20FB	326	17	-
CFB-10%	OPC+40FB	306	34	-
CFB-15%	OPC+60FB	276	51	-
CPS-5%	OPC+20PS	326	-	17
CPS-10%	OPC+40PS	306	-	34
CPS-15%	OPC+60PS	276	-	51

C:Cement; FB:Fly ash micro-beadsl; PS:phosphorus slag powder; fine aggragate=909; coarse aggregate=900; water=165; High performance water-reducing agent=5.88

3.8.1.SEM Analysis

Scanning Electron Microscopy (SEM) images of the different concrete samples are displayed in Figure 27.Figure 27(a) relates to the control sample cured for 7 days. It is observed that Calcium Hydroxide (CH) crystals are uniformly dispersed within the concrete matrix, and there are numerous micro-pores on the surface.Figure 27(b) shows the microstructure of the control sample after 28 days of curing. A significant amount of hydration products is visible in the sample, but some microscopic porosity still remains within the matrix.Figure 27(c) shows the microstructure of the sample containing 15% Fly Ash Microspheres (CFB-15%) after 7 days of curing. This image shows that the surface of the FB particles is covered with a layer of C-S-H gel, and CH is uniformly dispersed over the concrete substrate. The amount of hexagonal CH in this sample is significantly higher than in the control sample in Figure 27(a). At the same time, only a few micro-pores are observed on the surface of CFB-15%. The number of these pores is dramatically reduced compared to the control group, which is attributed to the significant filling effect of the fly ash microspheres and the slight reaction of FB with CH during the early stages of cement hydration.Figure 27(e) shows the SEM image of the sample containing 15% Phosphorous Slag (CPS-15%) after 7 days of curing. Due to the irregular surface shape of PS, proper granular distribution with cement particles is not

achieved, which increases micro-porosity in the cementitious matrix. The reaction between PS and CH is low in the early stages, as the amount of CH formed in the matrix is small.Figure 27(f) shows the SEM image of CPS-15% after 28 days of curing.

This image shows that PS has an irregular and solid shape. The adhesive bond between cement and PS particles is weaker than with FB. Even after 28 days of curing, some detrimental porosity remains in the structure because the filling effect of PS is not as effective as FB's. However, the amount of calcium silicate hydrate gel has increased significantly compared to day 7, leading to the increase in mechanical
strength at 28 days. [30]

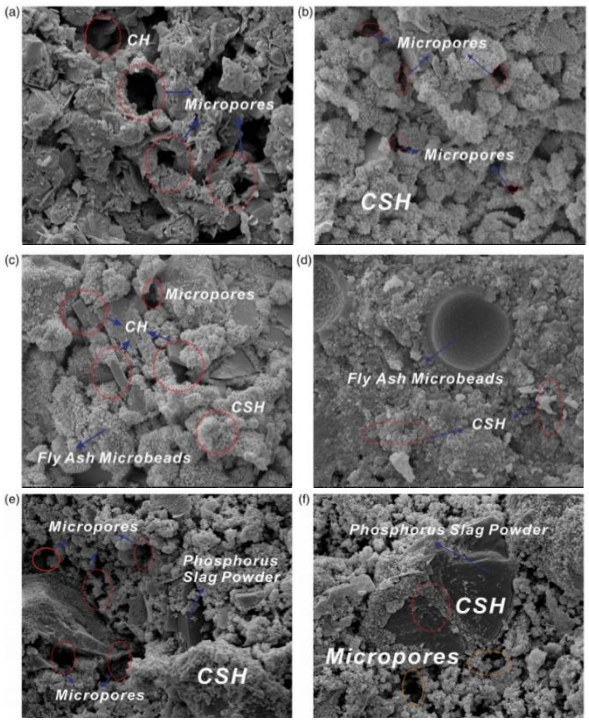

Figure 27. (a) SEM of the control specimen (7 days, 5000_). (b) SEM of the control specimen(28 days, 5000_). (c) SEM of the CFB-15% (7 days, 5000_). (d) SEM of the CFB-15% (28 days,5000_). (e) SEM of the CPS-15% (7 Days, 5000_). (f) SEM of the CPS-15% (28 Days, 5000_).

3.8.2.Compressive Strength

According to Figure 28, the compressive strength value was significantly higher compared to the reference sample. Therefore, adding Phosphorous Slag (PS) can severely reduce the early-age strength of self-compacting concrete compared to plain cement concrete, but it has little effect on long-term strength. The 7-day compressive strength of self-compacting concrete using Fly Ash Microspheres (FB) shows no significant change compared to plain cement concrete, indicating the higher early reactivity of FB compared to PS.

FB possesses high fineness, high purity, and an excellent filling effect as a micro-fine particle, even compared to PS. This characteristic allows FB to uniformly fill the spaces between cement particles, improving the pore structure of the concrete and resulting in a denser concrete.

As the cement hydration reaction progresses, the concentration of $Ca(OH)_2$ produced in the matrix gradually increases until it reaches saturation and $Ca(OH)_2$ crystals precipitate. [30]

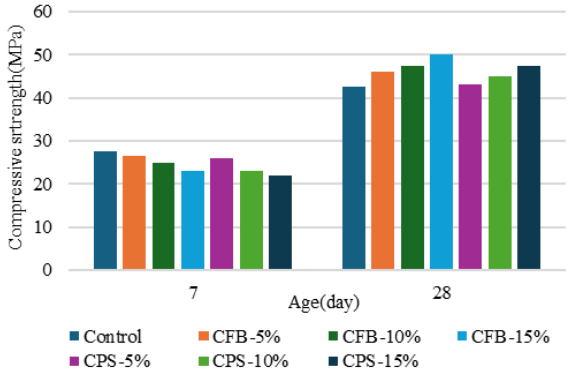

Figure 28. Compressive strength of specimens

3.9. High-Volume Fly Ash and Calcium Carbonate

This research investigates the properties of SCC mixed with different levels of Fly Ash (FA) and Calcium Carbonate powder (CC). Ordinary Portland Cement was replaced with FA at 20%, 30%, and 50% by weight, and with Calcium Carbonate at 5%, 10%, and 20% by weight. The total powder content was 550 kg/m³, and the water-to-binder ratio remained constant at 0.28 for all mixes. The SCC properties, including workability and the properties of various fresh and hardened concrete mixtures, were studied.

The results indicate that self-compacting concrete containing high volumes of ternary mixes with FA and CC meets the EFNARC standard requirements for filling ability, passing ability, and segregation resistance. Increasing FA and CC led to a decrease in unit weight, strength, and shrinkage, but increased the air content and water absorption. The highest compressive strength at 120 days exceeded 70 MPa. Furthermore, SCC mixes containing 70% [binder replacement?] had compressive strengths over 50 MPa. Microstructural analysis revealed that the calcium-silica ratio (CaO/SiO_2) played a role in increasing compressive strength, and the cost of SCC was reduced by 8 to 21 percent. Table 8 shows the nomenclature and mix design of each sample. [31]

Table 9.
Mixture proportions of materials used.

Mix	Cementitious materials(kg/m^3)			
	%replacement	Cement	Fly ash	Calcium carbonate
Control	0	550	-	-
20FA5CC	25	412.5	110	27.5
20FA10CC	30	385	110	55
20FA20CC	40	330	110	110
30FA5CC	35	357.5	165	27.5
30FA10CC	40	330	165	55
30FA20CC	50	275	165	110
50FA5CC	55	247.5	275	27.5
50FA10CC	60	220	275	55
50FA20CC	70	165	275	110

Water(kg/m3)=154, Fine aggregate (kg/m3)=815, Coarse aggregate (kg/m3)=720, HRWR(%)=2.2

3.9.1.SEM Analysis

SEM images of selected SCC mixes with different amounts of Fly Ash (FA) and Calcium Carbonate (CC) are shown in Figures 29a to 29d. The morphology of the control sample is seen in Figure 29(a), showing a significant amount of Calcium Hydroxide ($Ca(OH)_2$) and a moderate amount of Ettringite crystals within the hydrates, along with smaller pores. The SEM micrograph of the 20FA5CC sample is shown in Figure 29(b), which primarily consists of a relatively dense layer of hydrates and shows no significant difference from other mixes containing FA and CC. No large air-induced cracks or voids are visible.The 30FA10CC sample in Figure 29(c) has a weak Interfacial Transition Zone (ITZ) between the paste and aggregate, along with visible surface cracks. In contrast, the 50FA20CC sample (Figure 29(d)) shows a substantial amount of unreacted fly ash on the surface. The larger voids in the SCC mixes due to the addition of FA and CC indicate loose granular compounds and increased porosity near the interfacial zone; a small amount of Ettringite crystals is also observed within the hydrates. [31]

3.9.2.Compressive Strength

The results of the compressive strength test for Self-Compacting Concrete (SCC) at 7, 28, 60, and 120 days are shown in Figure 30. The control concrete has compressive strengths of 54, 56, 61, and 69 MPa at the respective ages. The trend of increasing compressive strength of SCC during the curing period shows that strength increases significantly with longer curing duration. However, a reduction in compressive strength occurs when cement is replaced with higher amounts of Fly Ash (FA) and Calcium Carbonate (CC). The development of compressive strength in concrete has an inverse relationship with the amount of FA and CC, as reducing the cement content and replacing it with powder materials affects the concrete's hydration reaction. Furthermore, CC and FA are very fine materials that increase water demand.

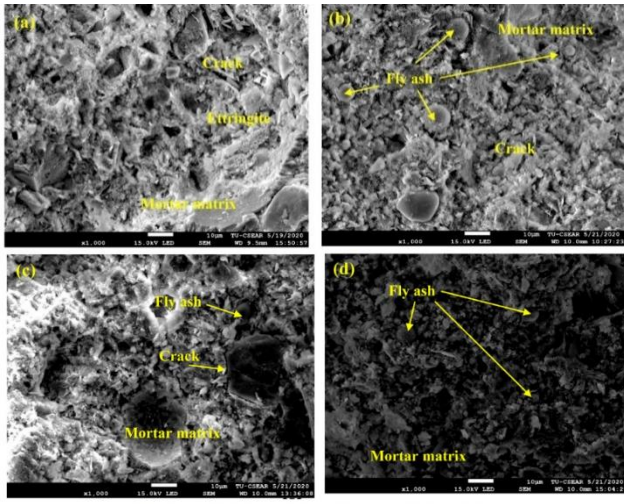

Figure 29. SEM micrographs of (a) Control (b) 20FA5CC (c) 30FA10CC and

When the water-to-binder ratio remains constant, the high water absorption by the cementitious materials reduces the chemical reaction between water and cement, consequently leaving voids in the hardened concrete which lower the compressive strength.There are three SCC mixes that exhibited higher compressive strength than the control concrete: 20FA5CC, 20FA10CC, and 30FA5CC, where the total cement replacement is equal to or less than 35%. However, when the cement replacement exceeds 40%, all mixes have lower compressive strength than the control sample because the mass of cement is replaced with FA and CC, which have lower density than cement.

This changes the paste volume relative to the aggregate grading and reduces the water-to-binder ratio (by volume); consequently, this ratio decreases as the cement replacement increases. In this study, the 50FA20CC mix has the lowest compressive strength, being 34%, 29%, 24%, and 17% lower than the control sample at 7, 28, 60, and 120 days, respectively. [31]

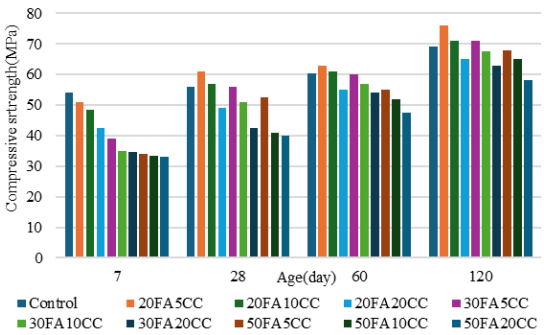

Figure 30. Compressive strength for all SCC mixes.

3.10.Class F Fly Ash, Circulating Fluidized Bed Combustion Fly Ash, and Ground Granulated Blast Furnace Slag

In the present study, the improvement of mechanical properties and durability of Cement-Free Self-Compacting Concrete (NC-SCC) with FFA was evaluated using experimental compressive strength tests. The experimental results indicated that adding 30% by weight of FFA as a partial replacement for slag was considered the optimal amount for producing cement-free self-compacting concrete with the highest mechanical properties, including compressive strength, dynamic modulus, and superior durability properties due to the lowest water absorption and volume of permeable voids calculated from the test on the initial and secondary rates of capillary water absorption. The microstructural performance, identified using Scanning Electron Microscopy (SEM), clearly showed that the structure of the Interfacial Transition Zone (ITZ) between the binder and aggregate in the NC-SCC appears to be strengthened by additional hydration products associated with the FFA particles when the optimal amount of FFA is added. Table 9 shows the nomenclature and mix design of each sample. [32]

Table 10.
Mixture proportions of NC-SCC

Mix code	Quantities (kg/m^3)				
	Water	GBFS	FFA	CFA	SP
SFC00	196	430	0	64	1.49
SFC10	193	382	42	64	2.62
SFC30	186	289	124	62	4.04
SFC50	182	201	201	60	3.31

FA=868, CA=853

3.10.1.SEM Analysis

To investigate the reactivity of Class F Fly Ash (FFA) in Cement-Free Self-Compacting Concrete (NC-SCC) mixtures, the internal microstructure of three hardened binders with different FFA contents—0% (mix SFC00), 30% (mix SFC30), and 50% by weight (mix SFC50)—is shown in Figures 31(a to c).

The micrograph in Figure 31(b), related to the SFC30 mix, shows that a very good bond is observed between the hydrated binder matrix and the aggregate surface. Furthermore, a typical Interfacial Transition Zone (ITZ) between the aggregate surface and the matrix was seen, with an approximate thickness of 8 to 12 micrometers, resulting from additional hydration products derived from the FFA particles, leading to a denser microstructure and higher compressive strength.In contrast, the micrographs in Figure 31(a) (mix SFC00) and Figure 31(c) (mix SFC50) showed weaker bonds between the hydrated binder matrix and the aggregate surface compared to Figure 31(b). Additionally, in the micrograph of Figure 31(c) (mix SFC50), several unhydrated FFA particles were observed, indicating that these unreacted particles create a porous structure, consequently leading to increased water absorption and reduced compressive strength. [32]

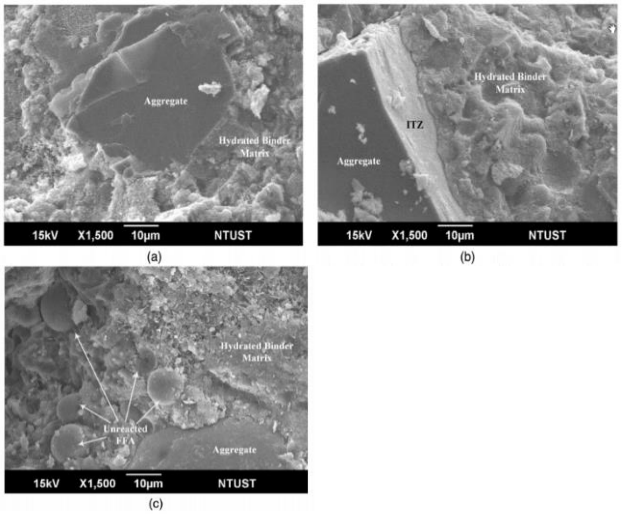

Figure 31. SEM micrographs of NC-SCC with different FFA amounts at age 28 days: (a) SFC00; (b) SFC30; and (c) SFC50

3.10.2.Compressive Strength

The effect of Class F Fly Ash (FFA) on the compressive strength development of Cement-Free Self-Compacting Concrete (NC-SCC) at 7 and 28 days was investigated, as shown in Figure 32. The results showed that mixtures with FFA added as a partial slag replacement at 10% and 30% by weight (mixes SFC10 and SFC30) increased the 28-day compressive strength by 16.67% and 19.56%, respectively, compared to the mix without FFA. However, the lowest compressive strength was observed in the mixture containing 50% by weight of FFA (mix SFC50). This was due to the high FFA content, which created a weak binding system because of the increased number of unhydrated FFA grains. [32]

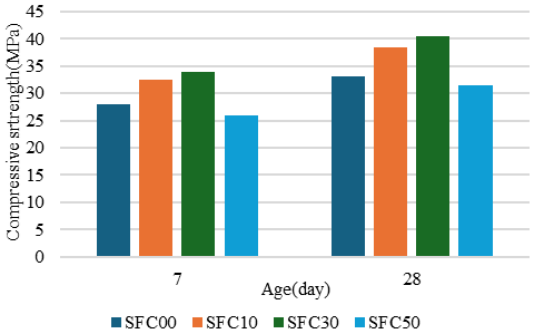

Figure 32. Influence of FFA on compressive strength of NC-SCC at ages 7 and 28 days.

3.11.Fly Ash and Red Mud

This study proposes using Red Mud (RM) for the partial replacement of Fly Ash (FA) (12.5, 25, and 50% by weight) in Self-Compacting Concrete (SCC) and investigates the effect of red mud on the fresh and hardened properties and the microstructural behavior of SCC. Slump flow, T500, and J-ring tests were conducted on the fresh SCC mixtures. The hardened properties of the red mud SCCs, including compressive strength, tensile strength, and modulus of elasticity, were studied. Furthermore, the chemical composition and microstructural properties of the red mud concrete samples were analyzed using X-ray Diffraction (XRD), Scanning Electron Microscopy (SEM), and Energy Dispersive X-ray Spectroscopy (EDS), respectively. The results indicate that the mechanical strength of the concrete increases with the amount of red mud. SCC specimens containing 50% red mud exhibited the best performance in terms of compressive strength and modulus of elasticity. The results from microscopic studies showed a slight improvement in the Interfacial Transition Zone (ITZ) between the aggregate and cement paste for the red mud concrete compared to the control concrete. XRD results revealed that the chemical composition of the cement paste containing red mud showed higher sodium and iron content. With increasing red mud content, some Albite crystals, appearing in triclinic form, were also identified by XRD. Table 10 shows the nomenclature and mix design of each sample. [33]

Table 11.
Concrete Mix Details (1 m3 concrete).

Mix code	Fly ash(kg/m^3)	Red mud (kg/m^3)	Super plastcizer (L)
Control	220	0	1.9
RMC12.5	192.5	27.5	2.5
RMC25	165	55.5	4.0(2.9)
RMC50	110	110	5.5(4.5)

w/b ratio =0.36, Water(kg/m^3)=195, Cement(kg/m^3)= 320, 10 mm aggregate (kg/m^3)=870, Beach sand (kg/m^3)=645

3.11.1.SEM Analysis

Scanning Electron Microscopy (SEM) was used to identify the characteristics of the hardened cement paste and the Interfacial Transition Zone (ITZ) between the cement paste and aggregates. The cement paste was visually examined to identify specific behaviors leading to incompatibility in the mix. Microcracks and incompatibilities might be the reason for abnormal strength increases or decreases in different mixtures. The crystalline structure of the cement paste was also identified.

The typical microscopic structure of the hardened cement paste in concrete containing red mud and the control concrete is shown in Figure 33. In general, a dense structure is observed due to the self-compacting nature of the concrete. The cement paste was examined for the presence of microcracks or unusual cracking patterns throughout the matrix.

In Figures 33a and 33b, the cement paste appears relatively uniform, and no significant cracks are observed. However, compared to RMC0, more voids were seen in the RMC12.5 mix, which might have caused the strength reduction at 56 days. The SEM image of the cement paste in RMC25 (Figure 33c) shows more microcracks than the other mixes, yet it does not appear more porous, as no significant dark areas are seen in the mix. This suggests that the gravel, sand, fly ash, and other materials are not well bonded together. In the RMC50 mix (Figure 33d), minor cracks were observed, similar in length and thickness to those in RMC25. These cracks are attributed to the high porosity of red mud, which increases water absorption and consequently reduces tensile strength, as tensile strength is more sensitive to this type of microcracking. It was observed that adding red mud can cause some microcracking in the concrete. [33]

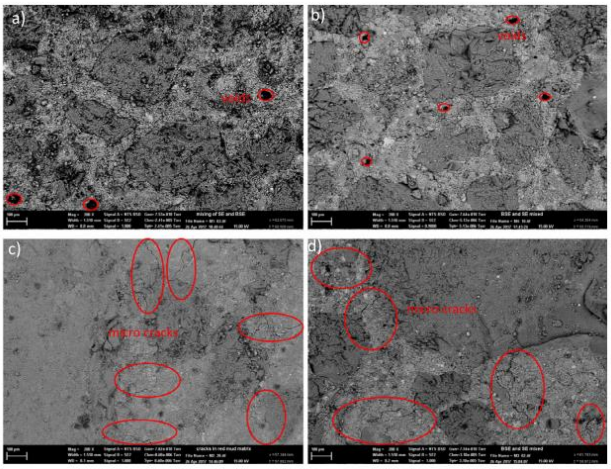

Figure 33. SEM images of cement paste: a) RMC0, b) RMC12.5, c) RMC25, d) RMC50.

3.11.2.Compressive Strength

The results of the compressive strength test are presented in Figure 34, where the horizontal lines represent the values of the control sample. It is observed that the strength development trend was very similar among the different mixes. The RMC0 mix had the lowest strength at all stages compared to the other mixes, except for RMC12.5 at 56 days. The overall trend of compressive strength at 56 days indicated an increase in strength with higher red mud content. It is evident that the most significant differences were related to the strength increase at 7 days, where the differences reached up to 13% for the 12.5% and 50% replacement levels. The primary reason for this is likely the

presence of a significant amount of Hatrurite (a mineral) in the cementitious structure, which will be discussed further. At 56 days, the compressive strength slightly increased with the amount of red mud, with a maximum difference of less than 4%. Therefore, it can be concluded that the effect of red mud content on compressive strength is not highly significant, but overall, the compressive strength values of the SCC mixes containing red mud were higher than those of the control concrete. [33]

4.Summary of Compressive Strength for All Specimens

Table 12 provides a summary of the compressive strength of all specimens mentioned in this study. All strengths listed in this table are for the age of 28 days to allow for an accurate comparison of the results. Furthermore, each specimen is compared to its respective control mix, and the percentage change in compressive strength is indicated in a separate column. The names used for each specimen correspond to the nomenclature from the original article, each of which can be found in the relevant section of this study.

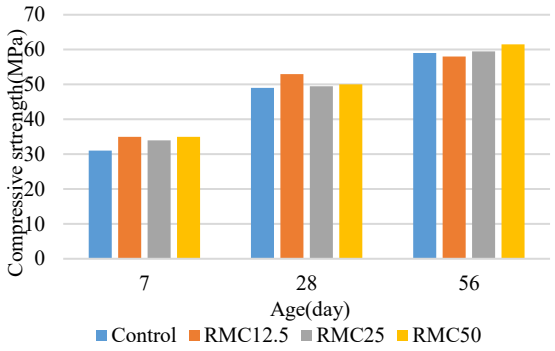

Figure 34. Comparison of compressive strength test results.

Table 12.
Summary of compressive strength of all samples

section	Mix ID code	Compressive strength	CONTROL	Percentage of changes
Fly Ash and Sodium Hydroxide	SCCF10	36.5	33.5	8.955223881
Fly Ash and Sodium Hydroxide	SCCF15	35.5	33.5	5.970149254
Fly Ash and Sodium Hydroxide	SCCF20	26	33.5	-22.3880597
Fly Ash and Sodium Hydroxide	SCCF25	11	33.5	-67.1641791
Fly Ash and Sodium Hydroxide	SCCF30	10	33.5	-70.14925373
Fly Ash, Silica Fume, and Metakaolin	SCCFA	24.5	23	6.52173913
Fly Ash, Silica Fume, and Metakaolin	SCCSF	23	23	0
Fly Ash, Silica Fume, and Metakaolin	SCCMK	27	23	17.39130435
Fly Ash, Metakaolin, and Hydrated Lime	B500FAHL	40.9	60.1	-31.94675541
Fly Ash, Metakaolin, and Hydrated Lime	B500FA	27.8	60.1	-53.7437604
Fly Ash, Metakaolin, and Hydrated Lime	B500FAM	32.6	60.1	-45.75707155
Fly Ash, Metakaolin, and Hydrated Lime	B500FAMHL	40	60.1	-33.44425957
Fly Ash, Metakaolin, and Hydrated Lime	B400FAHL	28.4	60.1	-52.74542429
Fly Ash, Metakaolin, and Hydrated Lime	B400FA	20	60.1	-66.72212978
Fly Ash, Metakaolin, and Hydrated Lime	NVC	32.1	60.1	-46.5890183
Fly Ash, Metakaolin, and Hydrated Lime	B400FAM	23	60.1	-61.73044925
Fly Ash, Metakaolin, and Hydrated Lime	B400FAMHL	27.5	60.1	-54.24292845
Fly Ash and Palm Oil Fuel Ash	FA10	67	73	-8.219178082
Fly Ash and Palm Oil Fuel Ash	FA20	63	73	-13.69863014
Fly Ash and Palm Oil Fuel Ash	TNY10	62	73	-15.06849315
Fly Ash and Palm Oil Fuel Ash	POFA10	59	73	-19.17808219
Fly Ash and Palm Oil Fuel Ash	FA30	54	73	-26.02739726
Fly Ash and Palm Oil Fuel Ash	TNY20	54	73	-26.02739726
Fly Ash and Palm Oil Fuel Ash	POFA20	54	73	-26.02739726
Fly Ash and Palm Oil Fuel Ash	TNY30	47	73	-35.61643836
Fly Ash and Palm Oil Fuel Ash	FA40	46	73	-36.98630137

Continued on next page

section	Mix ID code	Compressive strength	CONTROL	Percentage of changes
Fly Ash and Palm Oil Fuel Ash	TNY40	41	73	-43.83561644
Fly Ash and Palm Oil Fuel Ash	POFA30	38	73	-47.94520548
Fly Ash and Palm Oil Fuel Ash	POFA40	35	73	-52.05479452
Fly Ash and Blast Furnace Slag	GBFS30%	67.5	38.4	-3.571428571
Fly Ash and Blast Furnace Slag	GBFS40%	60.5	38.4	-13.57142857
Fly Ash and Blast Furnace Slag	GBFS50%	62.5	38.4	-10.71428571
Fly Ash and Blast Furnace Slag	GBFS60%	55	38.4	-21.42857143
Fly Ash and Blast Furnace Slag	GBFS70%	47	38.4	-32.85714286
Fly Ash, Silica Fume, and Marble	5SF	58	50.5	14.85148515
Fly Ash, Silica Fume, and Marble	10M	60	50.5	18.81188119
Fly Ash, Silica Fume, and Marble	20M	53	50.5	4.95049505
Fly Ash, Silica Fume, and Marble	30M	45	50.5	-10.89108911
Fly Ash, Silica Fume, and Marble	15FA	56	50.5	10.89108911
Fly Ash, Silica Fume, and Marble	15FA10M	63	50.5	24.75247525
Fly Ash, Silica Fume, and Marble	15FA20M	46	50.5	-8.910891089
Fly Ash, Silica Fume, and Marble	15FA30M	44	50.5	-12.87128713
Fly Ash, Silica Fume, and Marble	25FA	53	50.5	4.95049505
Fly Ash, Silica Fume, and Marble	25FA10M	58	50.5	14.85148515
Fly Ash, Silica Fume, and Marble	25FA20M	43	50.5	-14.85148515
Fly Ash, Silica Fume, and Marble	25FA30M	39	50.5	-22.77227723
Fly Ash, Silica Fume, and Marble	35FA	45	50.5	-10.89108911
Fly Ash, Silica Fume, and Marble	35FA10M	47	50.5	-6.930693069
Fly Ash, Silica Fume, and Marble	35FA20M	43	50.5	-14.85148515
Fly Ash, Metakaolin, Blast Furnace Slag	0.4M10	85	52	63.46153846
Fly Ash, Metakaolin, Blast Furnace Slag	0.4M20	89	52	71.15384615
Fly Ash, Metakaolin, Blast Furnace Slag	0.4G10	42	52	-19.23076923
Fly Ash, Metakaolin, Blast Furnace Slag	0.4G20	42.5	52	-18.26923077
Fly Ash, Metakaolin, Blast Furnace Slag	0.4G30	53	52	1.923076923
Fly Ash, Metakaolin, Blast Furnace Slag	0.4F10	28	52	-46.15384615
Fly Ash, Metakaolin, Blast Furnace Slag	0.4F20	29	52	-44.23076923
Fly Ash, Metakaolin, Blast Furnace Slag	0.4F30	32	52	-38.46153846
Fly Ash and Phosphorous Slag Powder	CFB5%	43	45	-4.444444444
Fly Ash and Phosphorous Slag Powder	CFB10%	47.5	45	5.555555556
Fly Ash and Phosphorous Slag Powder	CFB15%	50	45	11.11111111
Fly Ash and Phosphorous Slag Powder	CPS5%	46	45	2.222222222
Fly Ash and Phosphorous Slag Powder	CPS10%	45	45	0
Fly Ash and Phosphorous Slag Powder	CPS15%	45.5	45	1.111111111
Fly Ash and Calcium Carbonate	20FA5CC	60	57	5.263157895
Fly Ash and Calcium Carbonate	20FA10CC	57	57	0
Fly Ash and Calcium Carbonate	20FA20CC	49	57	-14.03508772
Fly Ash and Calcium Carbonate	30FA5CC	55	57	-3.50877193
Fly Ash and Calcium Carbonate	30FA10CC	51	57	-10.52631579
Fly Ash and Calcium Carbonate	30FA20CC	42	57	-26.31578947
Fly Ash and Calcium Carbonate	50FA5CC	53	57	-7.01754386

Continued on next page

section	Mix ID code	Compressive strength	CONTROL	Percentage of changes
Fly Ash and Calcium Carbonate	50FA10CC	42	57	-26.31578947
Fly Ash and Calcium Carbonate	50FA20CC	40	57	-29.8245614
Class F Fly Ash,Ground Granulated	SFC10	39	33.5	16.41791045
Class F Fly Ash,Ground Granulated	SFC30	40.5	33.5	20.89552239
Class F Fly Ash,Ground Granulated	SFC50	31.5	33.5	-5.970149254
Fly Ash and Red Mud	RMC12.5%	53	48.5	9.278350515
Fly Ash and Red Mud	RMC25%	49.5	48.5	2.06185567
Fly Ash and Red Mud	RMC50%	50	48.5	3.092783505

Figure 35 shows the eleven samples with the best effect on 28-day compressive strength.

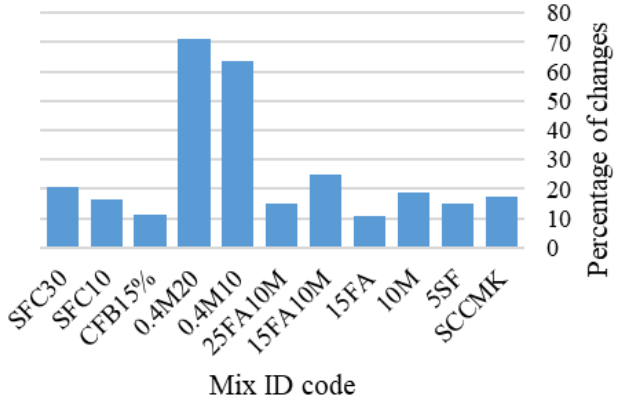

Figure 35. eleven samples with the best impact on compressive strength

5-Conclusion

Results from various studies indicate that fly ash, as an artificial pozzolan, plays a key role in improving the properties of SCC. Partial replacement of cement with FA, in addition to reducing cement consumption and costs, contributes to improved workability, reduced heat of hydration, and increased long-term stability and reduced permeability. However, the effect of FA on compressive strength and microstructure depends on the replacement level and the type of accompanying admixtures.

In general, the use of fly ash in combination with various admixtures has high potential for producing SCC with improved mechanical and microstructural properties. Selecting the optimal type and amount of admixtures, depending on the desired properties and environmental conditions, is of great importance. Admixtures such as metakaolin and silica fume, due to their high reactivity, contribute to improving early-age strength, while fly ash and blast furnace slag have a greater impact on long-term strength and durability.

Precise control of mix proportions and the curing process is essential to achieve the maximum benefits of these materials. Microstructural analysis using SEM provides a powerful tool for understanding the performance mechanisms of these admixtures and for optimizing self-compacting concrete mixtures.

Based on Table 12 and the points mentioned, the following specific results can be stated regarding the role of admixtures and fly ash:

[1] Fly Ash (FA), as an artificial pozzolan, improves the workability, stability, and permeability of Self-Compacting Concrete (SCC).

[2] Activating FA with Sodium Hydroxide (NaOH) enhances pozzolanic reactions and improves compressive strength at 10 to 15 percent replacement.

[3] Metakaolin (MK) significantly increases the early-age strength of SCC but exhibits the greatest strength loss at high temperatures.

[4] Silica Fume (SF) and MK undergo more severe microstructural degradation at high temperatures compared to FA.

[5] Hydrated Lime (HL), especially in combination with FA and MK, significantly increases compressive strength, particularly in low-cement concretes.

[6] Palm Oil Fuel Ash (POFA) performs less effectively than FA in replacing cement, but its optimized combination can be beneficial.

[7] Marble Cutting Slurry Waste (MCSW) combined with FA and SF creates a dense paste matrix and an improved Interfacial Transition Zone (ITZ) in SCC.

[8] Fly Ash Microspheres (FB), due to their high fineness and purity, have a better filling effect than Phosphorous Slag Powder (PS) and reduce porosity.

[9] The combination of FA and Calcium Carbonate (CC) with a total cement replacement of less than 35% can increase the compressive strength of SCC.

[10] Metakaolin (MK) has a greater effect on strengthening the microstructure of the Interfacial Transition Zone (ITZ) compared to Ground Granulated Blast Furnace Slag (GGBS) and significantly increases early-age strength.

[11] GBFS contributes to the improvement of SCC strength in the long term but may result in lower strength than the control concrete at early ages.

[12] Precise control of mix proportions and the curing process is essential to achieve the maximum benefits of admixtures in SCC.

References

[1] Okamura, H., & Ouchi, M. (2003). Self-compacting concrete. Journal of Advanced Concrete Technology, 1(1), 5-15. https://doi.org/10.3151/jact.1.5

[2] Scrivener, K. L., & Nonat, A. (2011). Hydration of cementitious materials, present and future. Cement and Concrete Research, 41(7), 651-665. https://doi.org/10.1016/j.cemconres.2011.03.026

[3] Bouzoubaâ, N., & Lachemi, M. (2001). Self-compacting concrete incorporating high volumes of class F fly ash: Preliminary results. Cement and Concrete Research, 31(3), 413-420. https://doi.org/10.1016/S0008-8846(00)00504-4

[4] Medina, C., Frías, M., & de Rojas, M. I. S. (2014). Leaching in concretes containing recycled ceramic aggregate from the sanitary ware industry. Journal of Cleaner Production, 66, 85-91. https://doi.org/10.1016/j.jclepro.2013.10.029

[5] Khayat, K. H., & Feys, D. (Eds.). (2010). Design, production and placement of self-consolidating concrete: Proceedings of SCC2010, Montreal, Canada, September 26-29, 2010 (Vol. 1). Springer Science & Business Media. https://doi.org/10.1007/978-90-481-9664-7

[6] Amziane, S., Crockett, N. J., Khayat, K. H., Sobolev, K., Brower, L. E., Domone, P. L., ... & Koehler, E. (2008). Report on measurements of workability and rheology of fresh concrete. American Concrete Institute.

[7] Van Eck, N., & Waltman, L. (2010). Software survey: VOSviewer, a computer program for bibliometric mapping. Scientometrics, 84(2), 523-538. https://doi.org/10.1007/s11192-009-0146-3

[8] Kumar, S., Murthi, P., Awoyera, P., Gobinath, R., & Kumar, S. (2022). Impact resistance and strength development of fly ash based self-compacting concrete. Silicon, 14(2), 481-492. https://doi.org/10.1007/s12633-020-00842-2

[9] Shen, W., Yang, Z., Cao, L., Cao, L., Liu, Y., Yang, H., ... & Bai, J. (2016). Characterization of manufactured sand: Particle shape, surface texture and behavior in concrete. Construction and Building Materials, 114, 595-601. https://doi.org/10.1016/j.conbuildmat.2016.03.201

[10] Saha, A. K. (2018). Effect of class F fly ash on the durability properties of concrete. Sustainable Environment Research, 28(1), 25-31. https://doi.org/10.1016/j.serj.2017.09.001

[11] Kanagaraj, B., Anand, N., Andrushia, D., Mathews, M. E., Alengaram, J., Arulraj, P., & Kiran, T. (2023). Mechanical properties and microstructure characteristics of self-compacting concrete with different admixtures exposed to elevated temperatures. Jordan Journal of Civil Engineering, 17(1), 1-9.

[12] Ye, G., Liu, X., De Schutter, G., Taerwe, L., & Vandevelde, P. (2007). Phase distribution and microstructural changes of self-compacting cement paste at elevated temperature. Cement and Concrete Research, 37(6), 978-987. https://doi.org/10.1016/j.cemconres.2007.02.011

[13] Sadrmomtazi, A., Gashti, S. H., & Tahmouresi, B. (2020). Residual strength and microstructure of fiber reinforced self-compacting concrete exposed to high temperatures. Construction and Building Materials, 230, 116969. https://doi.org/10.1016/j.conbuildmat.2019.116969

[14] Uysal, M., Yilmaz, K., & Ipek, M. (2012). Properties and behavior of self-compacting concrete produced with GBFS and FA additives subjected to high temperatures. Construction and Building Materials, 28(1), 321-326. https://doi.org/10.1016/j.conbuildmat.2011.08.076

[15] Mater, F. (2016). Influence of mineral admixtures on mechanical properties of self-compacting concrete under elevated temperature. Fire and Materials, 40, 940-958. https://doi.org/10.1002/fam.2354

[16] Anjos, M. A., Camões, A., Campos, P., Azeredo, G. A., & Ferreira, R. L. (2020). Effect of high volume fly ash and metakaolin with and without hydrated lime on the properties of self-compacting concrete. Journal of Building Engineering, 27, 100985. https://doi.org/10.1016/j.jobe.2019.100985

[17] Kupwade-Patil, K., Palkovic, S. D., Bumajdad, A., Soriano, C., & Büyüköztürk, O. (2018). Use of silica fume and natural volcanic ash as a replacement to Portland cement: Micro and pore structural investigation using NMR, XRD, FTIR and X-ray microtomography. Construction and Building Materials, 158, 574-590. https://doi.org/10.1016/j.conbuildmat.2017.09.165

[18] Tang, S. W., Cai, X. H., He, Z., Shao, H. Y., Li, Z. J., & Chen, E. (2016). Hydration process of fly ash blended cement pastes by impedance measurement. Construction and Building Materials, 113, 939-950. https://doi.org/10.1016/j.conbuildmat.2016.03.141

[19] Huo, Z., Xu, X., Lü, Z., Song, J., He, M., Li, Z., ... & Yan, L. (2012). Synthesis of zeolite NaP with controllable morphologies. Microporous and Mesoporous Materials, 158, 137-140. https://doi.org/10.1016/j.micromeso.2012.03.026

[20] Nagaratnam, B. H., Mannan, M. A., Rahman, M. E., Mirasa, A. K., Richardson, A., & Nabinejad, O. (2019). Strength and microstructural characteristics of palm oil fuel ash and fly ash as binary and ternary blends in Self-Compacting concrete. Construction and Building Materials, 202, 103-120. https://doi.org/10.1016/j.conbuildmat.2018.12.139

[21] Domone, P. L. (2007). A review of the hardened mechanical properties of self-compacting concrete. Cement and Concrete Composites, 29(1), 1-12. https://doi.org/10.1016/j.cemconcomp.2006.07.010

[22] Huseien, G. F., Sam, A. R. M., & Alyousef, R. (2021). Texture, morphology and strength performance of self-compacting alkali-activated concrete: Role of fly ash as GBFS replacement. Construction and Building Materials, 270, 121368. https://doi.org/10.1016/j.conbuildmat.2020.121368

[23] Huseien, G. F., Sam, A. R. M., Shah, K. W., Asaad, M. A., Tahir, M. M., & Mirza, J. (2019). Properties of ceramic tile waste based alkali-activated mortars incorporating GBFS and fly ash. Construction and Building Materials, 214, 355-368. https://doi.org/10.1016/j.conbuildmat.2019.04.154

[24] Mohammadhosseini, H., Lim, N. H. A. S., Tahir, M. M., Alyousef, R., Alabduljabbar, H., & Samadi, M. (2019). RETRACTED: Enhanced performance of green mortar comprising high volume of ceramic waste in aggressive environments. Construction and Building Materials, 212, 607-617. https://doi.org/10.1016/j.conbuildmat.2019.04.024 (Note: This article has been retracted).

[25] Huseien, G. F., Sam, A. R. M., Mirza, J., Tahir, M. M., Asaad, M. A., Ismail, M., & Shah, K. W. (2018). Waste ceramic powder incorporated alkali activated mortars exposed to elevated temperatures: Performance evaluation. Construction and Building Materials, 187, 307-317. https://doi.org/10.1016/j.conbuildmat.2018.07.226

[26] Huseien, G. F., Ismail, M., Tahir, M., Mirza, J., Hussein, A., Khalid, N. H., & Sarbini, N. N. (2018). Effect of binder to fine aggregate content on performance of sustainable alkali activated mortars incorporating solid waste materials. Chemical Engineering Transactions, 63, 667-672. https://doi.org/10.3303/CET1863112

[27] Choudhary, R., Gupta, R., & Nagar, R. (2020). Impact on fresh, mechanical, and microstructural properties of high strength self-compacting concrete by marble cutting slurry waste, fly ash, and

silica fume. Construction and Building Materials, 239, 117888. https://doi.org/10.1016/j.conbuildmat.2019.117888

[28] Dadsetan, S., & Bai, J. (2017). Mechanical and microstructural properties of self-compacting concrete blended with metakaolin, ground granulated blast-furnace slag and fly ash. Construction and Building Materials, 146, 658-667. https://doi.org/10.1016/j.conbuildmat.2017.04.158

[29] Asbridge, A. H., Page, C. L., & Page, M. M. (2002). Effects of metakaolin, water/binder ratio and interfacial transition zones on the microhardness of cement mortars. Cement and Concrete Research, 32(9), 1365-1369. https://doi.org/10.1016/S0008-8846(02)00798-6

[30] Deliang, H., Yu, S., Tianlu, L., Tao, W., Xiaodong, L., & Jinhua, Z. (2020). Mechanical and durability properties of self-compacting concrete made with fly ash microbeads and phosphorous slag powder. Journal of Adhesion Science and Technology, 34(14), 1572-1590. https://doi.org/10.1080/01694243.2020.1714136

[31] Promsawat, P., Chatveera, B., Sua-iam, G., & Makul, N. (2020). Properties of self-compacting concrete prepared with ternary Portland cement-high volume fly ash-calcium carbonate blends. Case Studies in Construction Materials, 13, e00426. https://doi.org/10.1016/j.cscm.2020.e00426

[32] Djayaprabha, H. S., Chang, T. P., Shih, J. Y., & Nguyen, H. A. (2020). Improving the mechanical and durability performance of No-cement self-compacting concrete by fly ash. Journal of Materials in Civil Engineering, 32(9), 04020245. https://doi.org/10.1061/(ASCE)MT.1943-5533.0003330

[33] Tang, W. C., Wang, Z., Liu, Y., & Cui, H. Z. (2018). Influence of red mud on fresh and hardened properties of self-compacting concrete. Construction and Building Materials, 178, 288-300. https://doi.org/10.1016/j.conbuildmat.2018.05.171